

MEASUREMENT OF FLAMMABILITY IN A CLOSED CYLINDRICAL VESSEL  
WITH THERMAL CRITERIA

A Dissertation

by

WUN K. WONG

Submitted to the Office of Graduate Studies of  
Texas A&M University  
in partial fulfillment of the requirements of the degree of

DOCTOR OF PHILOSOPHY

December 2006

Major Subject: Chemical Engineering

MEASUREMENT OF FLAMMABILITY IN A CLOSED CYLINDRICAL VESSEL  
WITH THERMAL CRITERIA

A Dissertation

by

WUN K. WONG

Submitted to the Office of Graduate Studies of  
Texas A&M University  
in partial fulfillment of the requirements of the degree of

DOCTOR OF PHILOSOPHY

Approved by:

Chair of Committee,	James C. Holste
Committee Members,	M. Sam Mannan
	Kenneth R. Hall
	Kalyan Annamalai
Head of Department,	N. K. Anand

December 2006

Major Subject: Chemical Engineering

## ABSTRACT

Measurement of Flammability in a Closed Cylindrical Vessel with Thermal Criteria.

(December 2006)

Wun K. Wong, B.S., Harvey Mudd College

Chair of Advisory Committee: Dr. James C. Holste

Accurate flammability limit information is necessary for safe handling of gas and liquid mixtures, and safe operation of processes using such mixtures. The flammability limit is the maximum or minimum fuel concentration at which a gas mixture is flammable in a given atmosphere. Because combustion occurs in the vapor phase, even in the case of liquids the flammability limits are applicable after calculating the vapor compositions. The body of flammability data available in the literature is often inadequate for use with the variety of conditions encountered in industrial applications. This is due to the scarcity of flammability data for fuel mixtures in non-standard atmospheric conditions, and inconsistencies in flammability values provided by different experimental methods.

This work reports on the design, construction and utilization of an apparatus capable of measuring flammability limits for a range of conditions including fuel mixtures, varying oxygen concentrations, and extended pressure and temperature ranges. The flammability apparatus is a closed cylindrical reaction vessel with visual, pressure and thermal sensors. A thermal criterion was developed for use with the apparatus based on observations of combustion behavior within the reaction vessel. This criterion

provides more detailed information about the combustion than is provided by the pressure criterion methods.

Measured flammability limits of several hydrocarbon mixtures in air compare well with limits obtained by open glass cylinder experiments, but not with the results of counterflow apparatus experiments. The current results show that Le Chatelier's rule describes the mixture results adequately. Minimum oxygen concentrations also were determined for methane, butane, and methane-butane mixtures and compared with values reported in the literature. Lower flammability limits were determined for an equimolar methane-butane mixture at varying oxygen concentrations.

Results show that the flammability data determined with thermal criteria has an acceptable level of accuracy. Recommendations for improving apparatus are made, based upon observations made while operating the flammability apparatus.

## ACKNOWLEDGEMENTS

I would like to thank my committee chair, Dr. Holste, and my committee members, Dr. Annamalai, Dr. Hall, and Dr. Mannan, for their guidance and support throughout the course of this research. I also thank Dr. Rogers for his guidance on experimental practices.

Also thanks to my friends and colleagues and the department faculty and staff, especially those in the May Kay O'Conner Safety Center, for a great experience at Texas A&M University. I also want to thank the Texas Advanced Technology Program, which provided the funding for this research.

Finally, thanks to my parents, for their support and encouragement.

## TABLE OF CONTENTS

	Page
ABSTRACT.....	iii
ACKNOWLEDGEMENTS.....	v
TABLE OF CONTENTS.....	vi
LIST OF FIGURES.....	viii
LIST OF TABLES.....	xi
1. INTRODUCTION.....	1
2. OBJECTIVES.....	3
3. PREVIOUS WORK.....	4
3.1 Overview.....	4
3.2 Flash points, flame points, and flammability limits.....	5
3.3 Common experimental methods.....	6
3.4 Method parameters and flammability.....	8
3.5 Standardization.....	11
3.6 New thermal criterion.....	14
4. EXPERIMENTAL APPARATUS.....	15
4.1 Overview.....	15
4.2 Reaction vessel with enclosure.....	18
4.3 Gas loading and mixing.....	23
4.4 Sensors.....	30
4.5 Igniter system.....	36
4.6 Safety analysis.....	40
5. METHODS AND PROCEDURES.....	45
5.1 Overview.....	45
5.2 Apparatus setup.....	45
5.3 Operating procedure.....	48
5.4 Flammability limit selection method.....	54

	Page
6. RESULTS AND DISCUSSION.....	57
6.1 Overview.....	57
6.2 Combustion types in reaction vessel.....	58
6.3 Thermistor signal and combustion zones.....	78
6.4 Thermal criterion for flammability.....	83
6.5 Flammability of hydrocarbons in air.....	85
6.6 Comparison of fuel mixture flammability limits with counterflow data.....	88
6.7 Flammability in atmospheres with reduced oxygen concentration.....	93
6.8 Summary.....	97
7. SUMMARY AND RECOMMENDATIONS.....	99
7.1 Summary.....	99
7.2 Recommendations.....	102
REFERENCES.....	105
VITA.....	109

## LIST OF FIGURES

FIGURE		Page
3.1	Experimental LFLs of fuel mixtures in air compared with Le Chatelier predictions.....	10
4.1	Reaction vessel design features.....	16
4.2	Reaction vessel mounted in the safety enclosure.....	19
4.3	Top flange of reaction vessel.....	20
4.4	Bottom flange of reaction vessel.....	21
4.5	Reaction vessel enclosure front view.....	22
4.6	Reaction vessel enclosure side-back view.....	23
4.7	Gas loading manifold and peripherals.....	24
4.8	Gas feed wall panel.....	25
4.9	External mixing system.....	27
4.10	Mixing vessel.....	28
4.11	Thermistor and fuse wire igniter positions relative to the reaction vessel top plate.....	33
4.12	Sample Wheatstone bridge circuit.....	34
4.13	Wheatstone bridge voltage as a function of thermistor temperature.....	35
4.14	Igniter system circuit.....	37
4.15	Igniter.....	39
4.16	Capacitor based igniter circuit.....	39
5.1	Video capture software control panel.....	46



FIGURE	Page
5.2 Labview control panel for pressure and temperature readings showing voltage as a function of time.....	47
5.3 Valve configuration for evacuating the mixing vessel, reaction vessel, and manifold.....	49
5.4 Valve configuration for loading fuel #1 into the mixing vessel.....	50
5.5 Valve configuration for manifold evacuation.....	51
5.6 Valve configuration for loading the test mixture into the reaction vessel.....	52
6.1 Images of non-propagation combustion in blank (air) experiment.....	59
6.2 Temperature and pressure profiles for non-propagation combustion....	61
6.3 Images of flash combustion.....	62
6.4 Temperature and pressure profiles for flash combustion.....	64
6.5 Images from discontinuous flame propagation .....	66
6.6 Temperature and pressure profiles for discontinuous flame propagation combustion.....	67
6.7 Images from continuous flame propagation.....	69
6.8 Temperature and pressure profiles for continuous flame propagation combustion.....	71
6.9 Temperature profiles for continuous flame propagation of ethylene.....	73
6.10 Comparison of signal profiles for thermistors 1 and 2.....	74
6.11 Pressure profile for continuous flame propagation of ethylene .....	75

FIGURE		Page
6.12	Images of continuous flame propagation of ethylene.....	76
6.13	Zones within the reaction vessel during combustion.....	78
6.14	Sample thermistor signal profiles: expanded flame and non- combustion.....	79
6.15	Sample thermistor signal profiles: termination (2).....	80
6.16	Sample thermistor signal profiles: termination (1).....	81
6.17	Double temperature peaks during combustion.....	82
6.18	Comparison of Le Chatelier predictions with experimental LFLs for methane/butane and methane/propane mixtures in air.....	91
6.19	Mixture LFL deviations from Le Chatelier's rule predictions.....	93
6.20	Experimental LFL of 50/50 methane-butane mixture within a reduced oxygen atmosphere.....	95
7.1	Recommended reaction vessel body setup.....	102
7.2	Recommended thermistor rack and new bottom plate setup.....	103

## LIST OF TABLES

TABLE		Page
6.1	Combustion of hydrocarbons in air at and near the flammability limit..	85
6.2	Lower flammability limits of hydrocarbons in air.....	86
6.3	Upper flammability limits of methane and ethylene.....	87
6.4	Combustion of methane/propane and methane/butane mixtures in air...	90
6.5	Combustion of methane, butane, and methane/butane mixture in atmosphere with reduced oxygen concentration.....	94
6.6	Comparison of minimum oxygen concentration values.....	96
6.7	Comparison of minimum oxygen concentration values found in previous works.....	97

## 1. INTRODUCTION

The safe handling of gas or liquid mixtures requires knowledge and understanding of their flammability. Industry deals with mixtures at various temperatures, pressures, oxygen concentrations, and other atmospheric conditions. Flammability data at those conditions is necessary for safe operation of processes.

Flash points are useful for liquid safety because they describe the temperatures at which a liquid develops flammable vapors. Regulatory agencies use flash point determinations produced by small-scale test apparatus to classify flammable liquids. Regulators provide guidance on transportation, handling, packaging, storing, dispensing, and protecting these materials based on these classifications [1]. They also require that flash points be provided as part of material safety data information. Flammability limits are often provided with material safety data sheets as well as flash points because they describe the composition of the gas that can form propagating flames. Because combustion occurs in the vapor phase, even in the case of liquids the flammability limits are applicable after calculating the vapor compositions. Knowledge of the flammability limits is more valuable for safety in design because it is applicable to liquids and gas mixtures.

---

This thesis follows the style of Journal of Hazardous Materials.

The body of flammability data available in the literature is often inadequate for use in the variety of conditions encountered in industrial applications. First, flammability limits for many pure substances at atmospheric conditions are generally available, but information for pure substances and mixtures in non-standard atmospheres or at pressures other than atmospheric are scarce. Models that predict the flammability limits of mixtures in non-standard conditions are particularly sought after, but their reliability is limited by the lack of experimental verification. Second, the usefulness of flammability data is reduced by inconsistencies between the results of different measurement methods. The differences are caused by a combination of environmental factors (size and shape of the apparatus, turbulence or flow scheme of the gas or mixture), source of ignition, and measurement criteria. Standardization of the experimental methods can minimize the inconsistencies in the body of flammability data. At the current state of the research, no such standards exist.

This dissertation deals with the construction and operation of an apparatus to examine and compare different measurement criteria, and to gather flammability data on some selected gas mixtures. The primary focus is on the feasibility and mechanics of using thermal criteria for the measurement.

## 2. OBJECTIVES

The first objective of this research is the design and construction of a flammability apparatus. Some design constraints include: sufficient size in the reaction vessel to reduce wall quenching, sufficiently fast gas loading and mixing to enable a large number of experiments in a reasonable time, and capability to utilize visual, pressure, and thermal criteria to detect flame propagation.

The second objective of this research is to examine the thermal criterion as a measurement of flame propagation. For open vessel apparatuses at atmospheric conditions, propagation is usually detected visually. Closed vessel apparatuses are capable of higher pressures, but the materials of construction make visual detection more difficult, and pressure criteria more often are used. Results from pressure and visual criteria experiments tend to differ significantly. Thermal criteria offer an alternative method for detecting flame propagation that is applicable in closed or open vessels. Examination of the experimental data will develop the analysis method for the thermal criterion. Also, comparisons between criteria can be made by collecting temperature, pressure and visual measurements simultaneously.

The third objective of this research is to determine the flammability limits of several hydrocarbon gases, as pure gases and as mixtures. The measurements for the pure gases serve to verify the apparatus. Mixture flammability limits serve to test the Le Chatelier model, which is accurate according to most experimental data, but not according counterflow experiments conducted recently [20].

### 3. PREVIOUS WORK

#### 3.1 Overview

Experimental work on flammability began as early as 1816, when Sir Humphrey Davy of England examined the flammability limits of methane by igniting methane-air mixtures in a narrow necked bottle out of concern for mine safety. In 1891, Le Chatelier [2] developed a mixing rule for determining the flammabilities of multiple fuel mixtures by relating flammabilities of mixtures to flammabilities of the pure components and their molar fractions. Since then, researchers have used a variety of methods to measure flammability, both of gases and liquids, to generate a body of flammability data for use in safety applications such as classification of chemicals, risk analysis, *etc.* Liquid flammability information generally is presented in terms of flash points or flame points, which can be determined by methods produced by the American Society for Testing and Materials (ASTM). Gas flammability information generally is given in terms of flammability limits, determined with several methods, including methods produced by the U.S. Bureau of Mines and the ASTM, as well as more recent European standard methods. The body of experimental data is complicated by the sometimes interchanged use of the similar but different terms “flash point” and “flame point”, and the inconsistent values of flammability limits determined with different methods. This presents a significant problem since various substance indices calculated from flammability limits would not contain information about the measurement method. The

users of these resources potentially can receive incorrect information, especially in the case where the fuel is a mixture.

### 3.2 Flash points, flame points, and flammability limits

Flash point as defined by ASTM is “the lowest temperature, corrected to a pressure of 760 mmHg at which application of an ignition source causes the vapors of a specimen to ignite under specified conditions of test” [3, 4]. Typical flash point measurements with ASTM methods involve heating a liquid sample in a cup to a test temperature. A pilot flame of hydrocarbon gas is passed over the liquid surface or vapor space of the liquid. Ignition is identified visually [4, 5].

Flame point (or fire point) is defined by the ASTM as “the lowest temperature at which a specimen sustains burning for a minimum of 5 s” [4]. The flame point is generally defined as the temperature at which the flame is self-sustained, usually slightly different than the flash point [6]. The sustained burning on top of a liquid is caused by downward propagation of the flame [7]. The difference between flash and flame point is simply that flame point refers to a self propagating flame, whereas the flash point only requires detectable ignition.

Flammability limits, sometimes referred to as explosion limits [8], are defined by ASTM as well as authors like Zabetakis and Britton as the fuel concentration in the mixture where a flame can propagate away from the ignition source in that mixture [3, 5, 9, 2]. When using this definition, it is possible to utilize flame point data to



approximate flammability limits by calculating the saturated vapor concentration of fuels at a given temperature, and *vice versa*. However, some researchers make no such distinction; instead they assume that the flash point vapor concentration is the flammability limit [10], a practice that causes some confusion in interpreting values reported in the literature. In addition, flammability limits are divided into two types: the upper flammability limit (UFL) where the fuel concentration becomes too rich to be ignited and a lower flammability limit (LFL) where the fuel concentration becomes too lean to be ignited. Flash and flame points can be used to calculate the approximate LFL of a chemical, as they represent temperatures where barely enough fuel is in the vapor phase for combustion. The UFL cannot be approximated using flash and flame points for this reason. Attempts to relate flash and flame point data to flammability limits are further complicated by different experimental conditions and criteria that arise with different methods. Flammability limits can be affected by temperature, pressure, direction of flame propagation, and other environmental factors such as shape, size, or material of reaction vessel, ignition type, ignition energy, *etc.* [8, 9, 11]. The following section provides background on the current and past state of research methods.

### 3.3 Common experimental methods

The U.S. Bureau of Mines generated a large body of flammability data for pure gases, as well as some gas mixtures. Much of the work was done and summarized by Coward and Jones *et al.*, Zabetakis *et al.*, and Kuchta *et al.* [8, 12, 13] through Bureau of

Mines Bulletin publications. Flammability limits usually were determined by visual identification of flame propagation away from the point of ignition. Most of the measurements were made on premixed, quiescent gases in glass cylinders that were open at the bottom. The criterion for flammability is flame propagation from the bottom of the cylinder (ignition end) to the top of the cylinder (1 to 1.5 m in length). More recent experiments with a similar objective of measuring vertical flame propagation involve the use of an open bottomed steel cylinder with a thermocouple at the top for flame detection [14, 15].

Apparatus with closed, steel, spherical (and near spherical) reaction vessels and center ignition also have been used for flammability limit determinations in recent years. Unlike glass cylinders the visual detection of flames cannot be accomplished without a port, so the detection criterion usually is the relative pressure increase resulting from combustion. In these types of experiments there is no standard pressure rise criterion or vessel size. Burgess in 1982 published data from a 25,500 L sphere (3.65 m I.D.) that incorporated a 7 % pressure rise criterion in addition to the visual detection of flame propagation [16], and Cashdollar in 2000 published data [17] from 20 L (0.337 m I.D.) and 120 L (0.612 m I.D.) chambers with 3 or 7 % pressure rise criterion as well as reviewed older data from 8 L (0.248 m I.D.) and 25,500 L chambers.

Flammability limits also have been determined indirectly using counterflow burners, where twin gas jets of premixed fuel and oxidizer are released from opposing nozzles against each other, and ignited to produce twin, planar flames. The stretch rate, defined as the average gas exit velocity and half the distance between the nozzles, is

measured at different fuel concentrations. The fuel concentration is plotted as a function of stretch rate. The fuel concentration is extrapolated linearly to a stretch rate of zero, and this intercept is taken as the flammability limit [18]. This method is known to determine flammability limits of lower hydrocarbons at values similar to those found with spherical vessels, though it is suggested that the relationship between flame stretch and flammability limit is not strictly linear, and might fail to determine a correct limit under some conditions [19].

### 3.4 Method parameters and flammability

Parameters that influence flammability limits can be described roughly by the following groups: attribute of the apparatus (*e.g.* shape, size, ignition source power, ignition location), physical condition of the gas mixture (*e.g.* temperature, pressure, turbulence), and operator (criterion for flammability, accuracy) [8]. While any of those parameters can affect the flammability limit measured, usually the physical condition of the gas mixture is a characteristic of the chemical being investigated. It is the apparatus and the operator parameters that are specified by an experimental method. For methods with a reaction vessel that contains the gas mixture, vessel size and shape, ignition power and location, and flammability criteria are especially important. Flame propagation requires sufficient heat transferred from the flame to the unburned gas surrounding it, thus anything that reduces the available energy will affect the limits [12]. Vessels with greater distance between the walls and the ignition source, as well as larger

diameters therefore tend to have wider flammability limits ( lower LFLs, higher UFLs) as the quenching effects are reduced. The power of the ignition source must be sufficiently large to induce consistent ignition, but not so large that spurious indications of propagation are observed [2]. The choice of criteria also must take the other factors into consideration. For example, flame propagation in a cylinder with bottom ignition tends to cause a greater pressure increase than in an equivalent cylinder with center ignition. This occurs because downward propagation of flames is less likely near the flammability limit and a greater amount of gas will combust if ignited at the bottom. The pressure rise criterion needs to be larger for this setup to address the difference.

Counterflow apparatuses do not share apparatus parameters such as vessel shape, size, or ignition energy with other apparatuses. Instead, the key parameters are nozzle size and nozzle distance, because the method measures stretch rates from already burning twin jet flows of gas.

In some cases, inconsistent flammability values result from the differences in the methods. A recent study on the lower flammability limits of methane-ethane and methane-propane mixtures using a counterflow apparatus yields significantly different values than those predicted by Le Chatelier's rule [20]. This contradicts previous work by Coward *et al.* [21] that shows methane-ethane, methane-propane, and methane-butane mixtures obey Le Chatelier's rule closely. Figure 3.1 shows the experimental and predicted values of methane-ethane and methane-propane lower flammability limits. Additional measurements are required to resolve this contradiction.

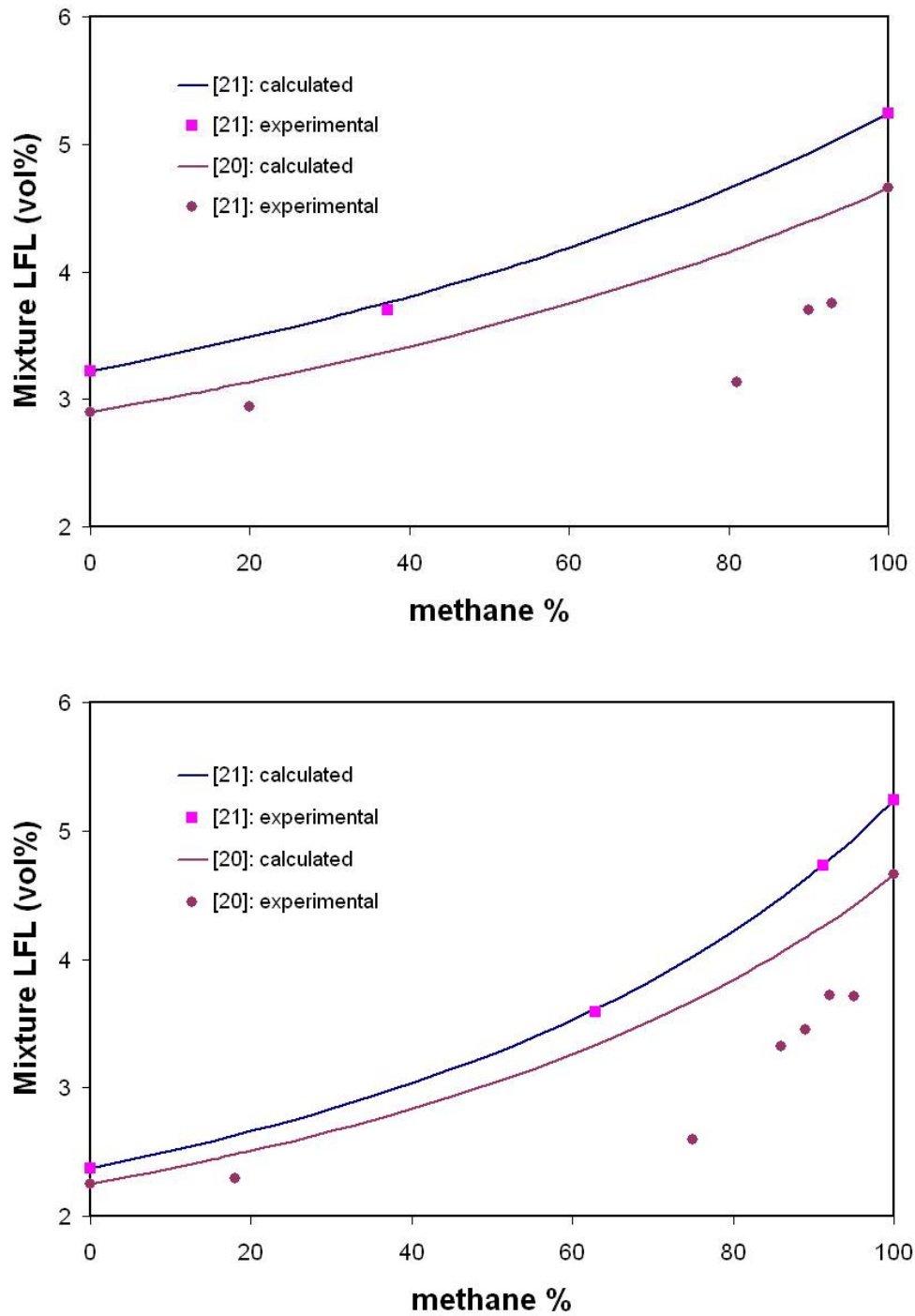


Fig. 3.1 Experimental LFLs of fuel mixtures in air compared with Le Chatelier predictions. Methane-ethane (top) and methane-propane (bottom) mixtures in air.

### 3.5 Standardization

There have been many attempts to standardize the measurement methods to improve compatibility of flammability data. ASTM adopted three closed vessel methods for gas and vapors: a general method (ASTM E 681-01), a specific method for gases and vapors at varying oxygen content (ASTM E 2079-01), and a specific method for chemicals at elevated temperature and pressure (ASTM E 918-83). ASTM E 681-01 uses a 5 L glass sphere with a high voltage, central spark as the ignition source. Flame propagation is defined as an upward and outward movement of the flame front from the ignition point, which adds the important feature that the flame is required to show self propagation independent of the plume of hot gas created by the ignition source [22]. ASTM E 2079-01 requires a 4 L or larger near-spherical vessel with a 10 J or greater ignition source, and a 7 % total pressure rise (with adjustment due to ignition effects) criterion [23]. E 918-83 requires a 1 L and 76 mm diameter minimum vessel inside an insulated oven with a fuse wire igniter near the bottom, and a 7 % total pressure rise criterion [24].

The current European standard methods for flammability limit determination are the DIN 51649 and EN 1839 methods. The DIN 51649 test method uses a 6 cm diameter, 30 cm tall glass cylinder opened at the top, with a spark igniter (0.5 s, at 10 W) at the bottom. The criterion for flammability is any visual sign of flame detachment from the ignition source. The EN 1839 method has both an open cylinder method and a closed vessel method, generally referred to as EN 1839 (T) and EN 1839 (B)

respectively. The EN 1839 (T) method uses a 8 cm wide, 30 cm tall, open top glass cylinder, with spark igniter at the bottom (0.2 s, at 10 W). The criterion for flammability is propagation of the flame 10 cm vertically above the igniter or 12 cm in the horizontal direction at any point of the flame path. EN 1839 (B) allows the use of a cylindrical or spherical vessel of at least 5 L and an exploding fuse wire (0.2 s, at 10 to 20 J) in the center. The criterion for flammability is a 5 % minimum pressure rise after ignition [25].

These attempts at standardization have achieved only limited success. ASTM E 681-01 has not been used widely, as most spherical vessel experiments use vessels larger than 5 L, and the pressure criterion instead of visual observation. The ideal pressure criterion is also ambiguous as the 7 % and 5 % criteria specified by the ASTM and European standards respectively differ, and different fuels have different pressure rise characteristics. For example, some refrigerants have a pressure rise of only 2 % when a propagating flame is ignited [26]. Researchers also continue to use counterflow methods, as well as other methods to determine flammability. A survey done by Britton [2] shows that the closed vessel methods with pressure criteria tend to have wider flammability limits than the open cylindrical vessel methods done by the U.S. Bureau of Mines. DIN 51649 and EN 1839 (T) tend to have much wider limits than other sets of data as well, possibly because their criterion only require short flame propagation distances. Moreover, the European definition of flammability is different from the American definition. The American standards and authors define flammability limits as the limiting fuel concentrations where the flame propagates through the mixture, while the European definition is the limiting concentration where the flame just fails to

propagate [25]. The difference in definitions and the effect of the less stringent criteria of short flame propagation distance and 5 % pressure rise instead of 7 % widens the flammability limits determined by DIN 51649-1 and EN 1839.

There is no universally accepted standard procedure for flammability determination. In 2002, Britton [2] reviewed the state of flammability research and made the following recommendations:

- Flammability limits should be measured to approximate free flame propagation independent of quenching effects by the walls or overdriving by the ignition source.
- The body of data using the American definition of flammability and European definition of flammability should not be mixed, and if they are compiled together the difference in definition should be noted.
- Experiments should be conducted in large diameter cylindrical apparatus, with bottom ignition, and a 7 % pressure rise criterion. This set of parameter can reduce the effect of quenching, and increase the pressure rise for more consistent results.

While the recommendations by Britton are based on reasonable assessments, experience showed that different pressure rise criteria than 7 % must sometimes be used to determine consistent flammability limits with different test vessels [8, 26, 27, 28].



### 3.6 New thermal criterion

This work uses an alternative criterion for flammability determination.

Thermistors at multiple locations above the ignition point can be used to track flame propagation in a cylindrical or spherical vessel. In this work we compare this thermal criterion with pressure and visual criteria, and flammability limits found by this method with those reported in the literature. The vessel used for this work has a closed cylindrical geometry, based on the recommendation by Britton [2].

## 4. EXPERIMENTAL APPARATUS

### 4.1 Overview

The flammability apparatus is a device used to detect flammability limits of gas mixtures. The key design features of the apparatus include:

1. Operational safety
2. Practical operation and maintenance by one individual
3. Multiple methods to detect combustion
4. Sufficient reaction vessel size to minimize flame quenching effects
5. Sufficient distance between igniter and sensor to minimize spurious results caused by ignition effects
6. Short turnaround time between experiments
7. Sufficiently fast data acquisition system to capture detailed time profiles of sensor measurements

The primary apparatus design features include: vessel shape, vessel size, ignition type, ignition location, and sensor locations.

The reaction vessel shape is a closed cylinder. Britton [2] recommended this geometry partly for ease of maintenance, but mostly because when combined with bottom ignition the pressure rise will be relatively large so that a pressure criterion easily can be applied. The geometry is also similar to that of the apparatus used by the U.S. Bureau of Mines and the more recent European standard EN 1839 (T). Determination of flammability limits similar to those standards; some propagation (10 cm vertical) away

from ignition source, or propagation to the top of the cylinder is likely to produce similar values, allowing for apparatus validation by comparison. Figure 4.1 shows schematically the reaction vessel with design features.

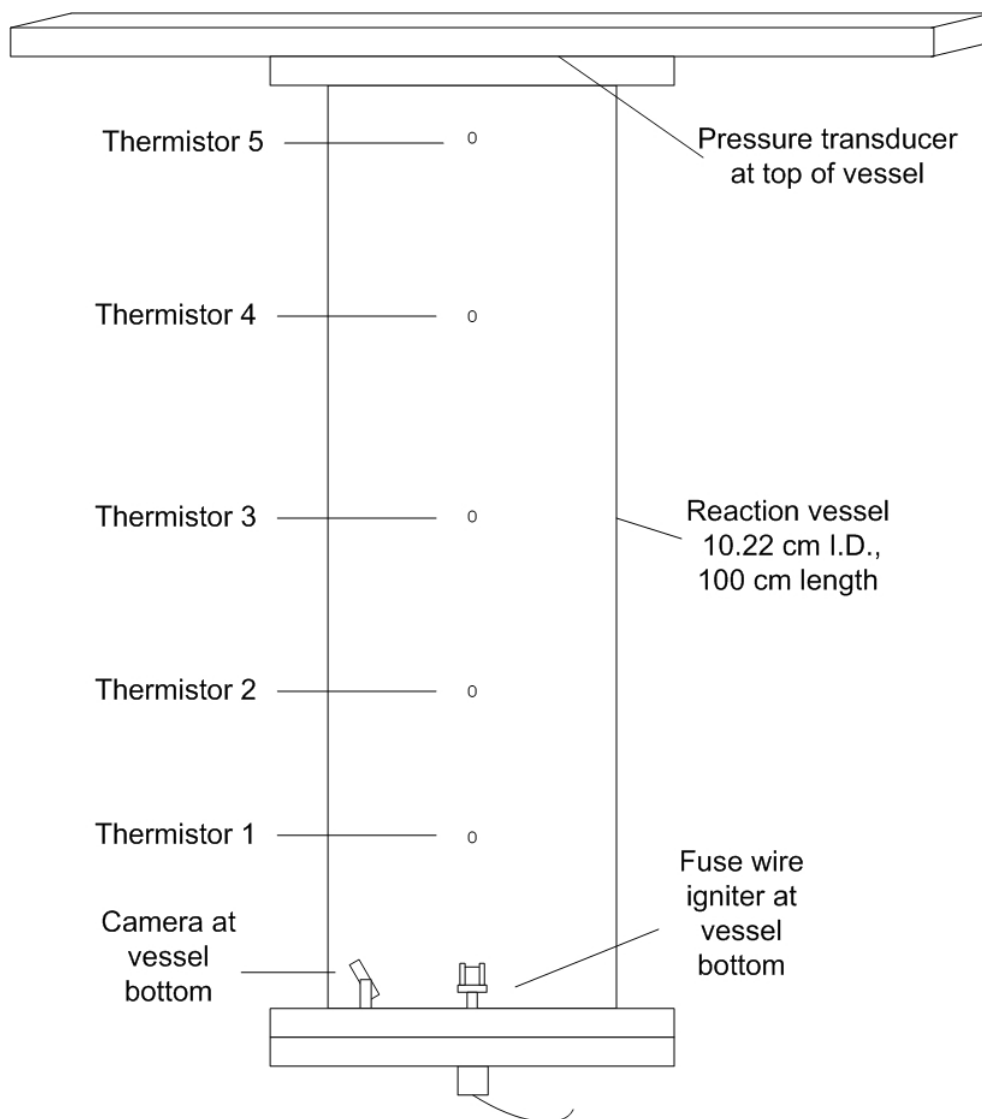


Fig. 4.1. Reaction vessel design features.

While the recommended size for such a vessel is 30 cm diameter, 100 to 150 cm long [2] or 30 cm diameter and 60 cm long [11], a stainless steel vessel of such size with sufficient pressure rating would be far too heavy for one person to handle, presenting safety and practical issues during maintenance. The vessel interior dimension chosen is approximately 10 cm in diameter and 100 cm in length, which results in a much lighter reactor vessel. Previous work has shown that reaction vessels with similar dimension have sufficient width to minimize quenching of typical fuel flames and sufficient distance between the igniter and the pressure sensor at the top of the vessel to minimize ignition energy effects on the measurement results [27].

The ignition source should provide enough energy to start the combustion process, but not too much additional energy. The most commonly used ignition sources reported in the literature are fuse wires and electrical arcs (sparks), but fuse wire has a greater power density and therefore imparts more useful heat into the gas mixture [2]. Furthermore, Mashuga [29] demonstrated that fuse wire explosions can have a consistent pattern of energy and power input, thus improving the repeatability of an experimental parameter. Therefore this apparatus uses an exploding fuse wire as the ignition source.

The type of measurements needed for flammability detection are visual, pressure and thermal. Thermal detection of flame along the vessel center can determine flame propagation. Visual and pressure measurements can confirm the thermal detection results. The thermal sensors are placed along the center axis of the vessel body to provide the most sensitive detection of flames and to minimize wall effects. The pressure sensor is located at the top of the vessel to minimize effects of the ignition

source on the measurements. The visual sensor is at the bottom of the vessel, allowing it to verify proper fuse wire explosions, and also to confirm instances of short flame propagation away from the igniter where the flame front does not reach the top of the vessel.

#### 4.2 Reaction vessel with enclosure

The reaction vessel consists of three major sections, the top plate, the reactor body, and the bottom plate. The top plate is affixed permanently to the vessel enclosure, and the reactor body and bottom flange hang from it when assembled. The reactor body is a schedule 40, 4 inch nominal (11.43 cm O.D., 10.22 cm I.D.), 100 cm long, stainless steel (SS 316) cylinder with welded flanges (7.78 cm O.D., 1.778 cm thick, 12 threaded bolt holes). A clamp near the midpoint of the reactor body connects it to a counterweight pulley system that provides ease of handling during maintenance. The bottom plate and the top plate bolt directly to the reactor body. The vessel is sealed against vacuum and pressure with O-rings (Viton<sup>®</sup>, 10.76 cm I.D. 0.262 cm width) between flanges and top and bottom plates. The reaction vessel has a volume of 8.2 L. Figure 4.2 shows the reaction vessel mounted on the enclosure.



Fig. 4.2. Reaction vessel mounted in the safety enclosure.

The top plate is a 1.905 cm thick, 20.32 cm wide, 60.96 cm long stainless steel plate with ports for the pressure transducer, thermistor signal feedthroughs, and the gas loading/relief valve section. Two holes on the top plate allow steel cables through to the clamp on the reactor body to the counterweight system above. Figure 4.3 shows the top plate.

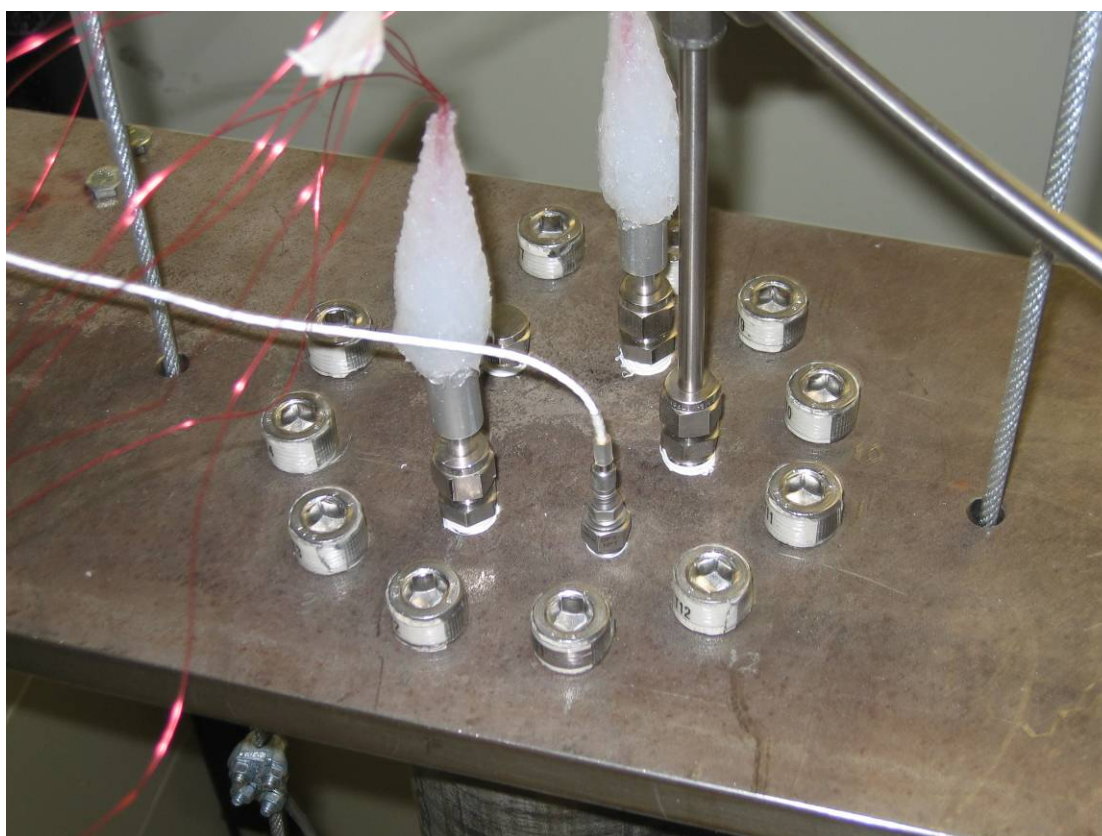


Fig. 4.3. Top flange of reaction vessel.

The bottom plate is an 1.778 cm thick, 17.78 cm diameter stainless steel flange with a large center port for igniter insertion, a port connecting to the signal/power

feedthrough for an internal camera and a spare port (currently unused). Figure 4.4 shows the bottom of the reaction vessel.

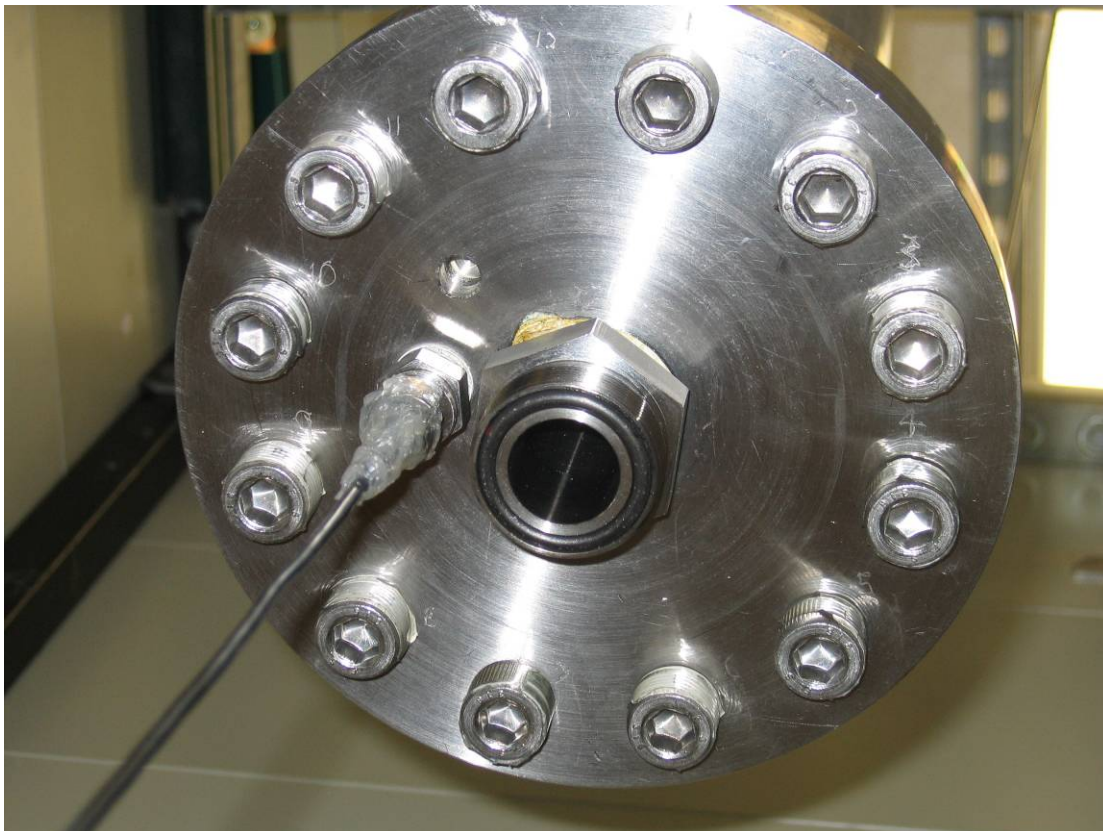


Fig. 4.4. Bottom flange of reaction vessel.

The reaction vessel enclosure is a rectangular structure built of Unitstrut<sup>®</sup> components, with 1 5/8 inch square struts forming the frame. The vessel is accessible through two hinged half-door sections that swing outward, allowing full access and partial access during igniter disengagement for fuse wire replacement. Two of the walls are constructed of 1/8 in thick steel sections riveted together. The third wall and the



hinged sections are covered with 2 layers of  $\frac{1}{4}$  in thick Lexan<sup>®</sup> sheets. Figure 4.5 shows the front view of the enclosure with the half-doors closed. Figure 4.6 shows a side view of the enclosure from a steel wall side.



Fig. 4.5. Reaction vessel enclosure front view.



Fig. 4.6. Reaction vessel enclosure side-back view.

The components for the reaction vessel and enclosure were constructed by the Texas A&M chemical engineering department machine shop. The design and safety analysis of the reaction vessel are addressed in a later section.

#### 4.3 Gas loading and mixing

The gas mixtures used with the experimental apparatus are synthesized by loading the individual components from the pressurized cylinders in which they are

supplied into an external mixing device through a gas loading manifold. After mixing is complete, the test mixtures are loaded into the reaction vessel through the manifold.

Figure 4.7 shows schematically the gas loading manifold and peripherals for the flammability apparatus.

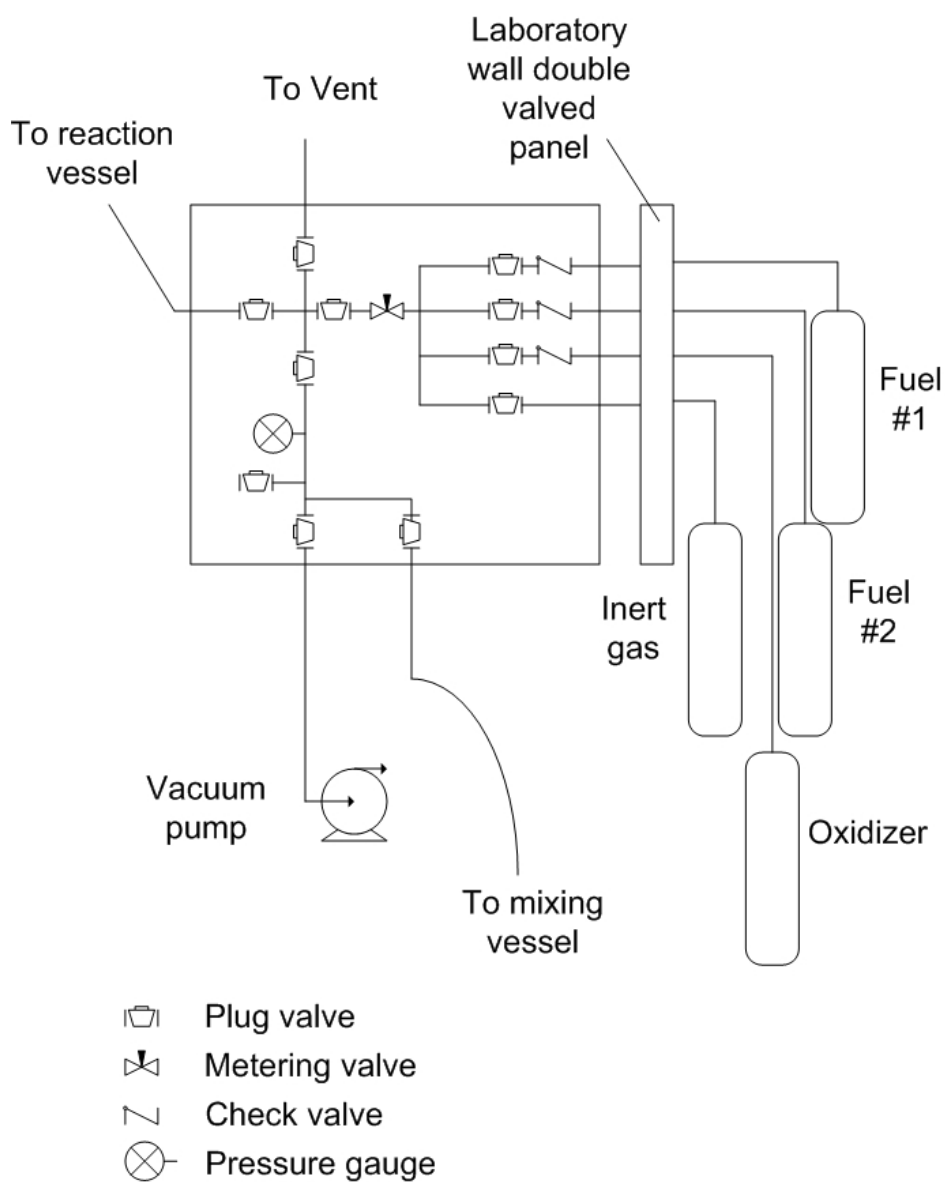


Fig. 4.7. Gas loading manifold and peripherals.

The gas loading system begins at the pressurized cylinders stored in the chemical storage hallway adjacent to the laboratory. Each pressurized cylinder connects to an appropriate pressure regulator, then through the double valve gas feed wall panel (built-in feature of laboratories in the Jack E. Brown Texas A&M Engineering Building) into the laboratory area. Figure 4.8 shows the wall panel from the laboratory side (the arrangement in the storage hallway is identical).



Fig. 4.8. Gas feed wall panel.

The fuel lines and the oxidizer line connecting to the gas loading manifold all contain check valves to prevent reverse gas flow if valve failure or operator error occurs. The check valves (Swagelok<sup>®</sup>) have 6,000 psig maximum working pressure and 4 psid cracking pressure. The combined gas line from all pressurized cylinders includes a metering valve leading to a cross junction that connects to four sections: the external mixer, the reaction vessel, the vacuum pump (Welch Mfg. DuoSeal Pump, ultimate vacuum:  $1.4 \times 10^{-3}$  mm Hg from department tests), and the vent line. The junction area has a pressure transducer (Omega PX603, 0.4 % accuracy with 0.04 %/F thermal zero and span effect) that provides pressure information for gas loading to specified pressures, and plug valves that allow isolation of each section from the gas line and each other. The manifold is purged with inert gas (nitrogen) and evacuated between each gas loading step. The vent line releases the contents from the manifold, as well as the reaction vessel and the mixer during different stages of gas loading, directly into a constant suction laboratory vent to prevent the build up of flammable gases in the laboratory. All gas lines (1/4 in tubing, 0.028 in thick) and valves (Swagelok<sup>®</sup>, Nupro<sup>®</sup>, or Cajon<sup>®</sup>) in the manifold are stainless steel (Type 316) with Swagelok<sup>®</sup> compression fittings. Detailed specifications are discussed in a later section.

The external mixer imitates the mixing scheme from a portable sample cylinder designed by Precision General Inc. (patents: 4,862,754; 4,930,361; 5,109,712). The mixing vessel is a cylinder that contains a cylindrical Teflon<sup>®</sup> block that slides along the length of the vessel. The block diameter is slightly smaller than the cylinder internal diameter, allowing smooth movement of the block. When the vessel is rotated, the block

falls toward the lower end. Gases moving between the block and the vessel wall create highly turbulent zones in front of and behind the moving block. These zones facilitate fast mixing of the gases. The external mixer consists of a mixing vessel and a motor for vessel rotation, both mounted on top of the mixing stand (made of 1.25 in square steel tubing welded together). Figure 4.9 shows the external mixer assembly.



Fig. 4.9. External mixing system.

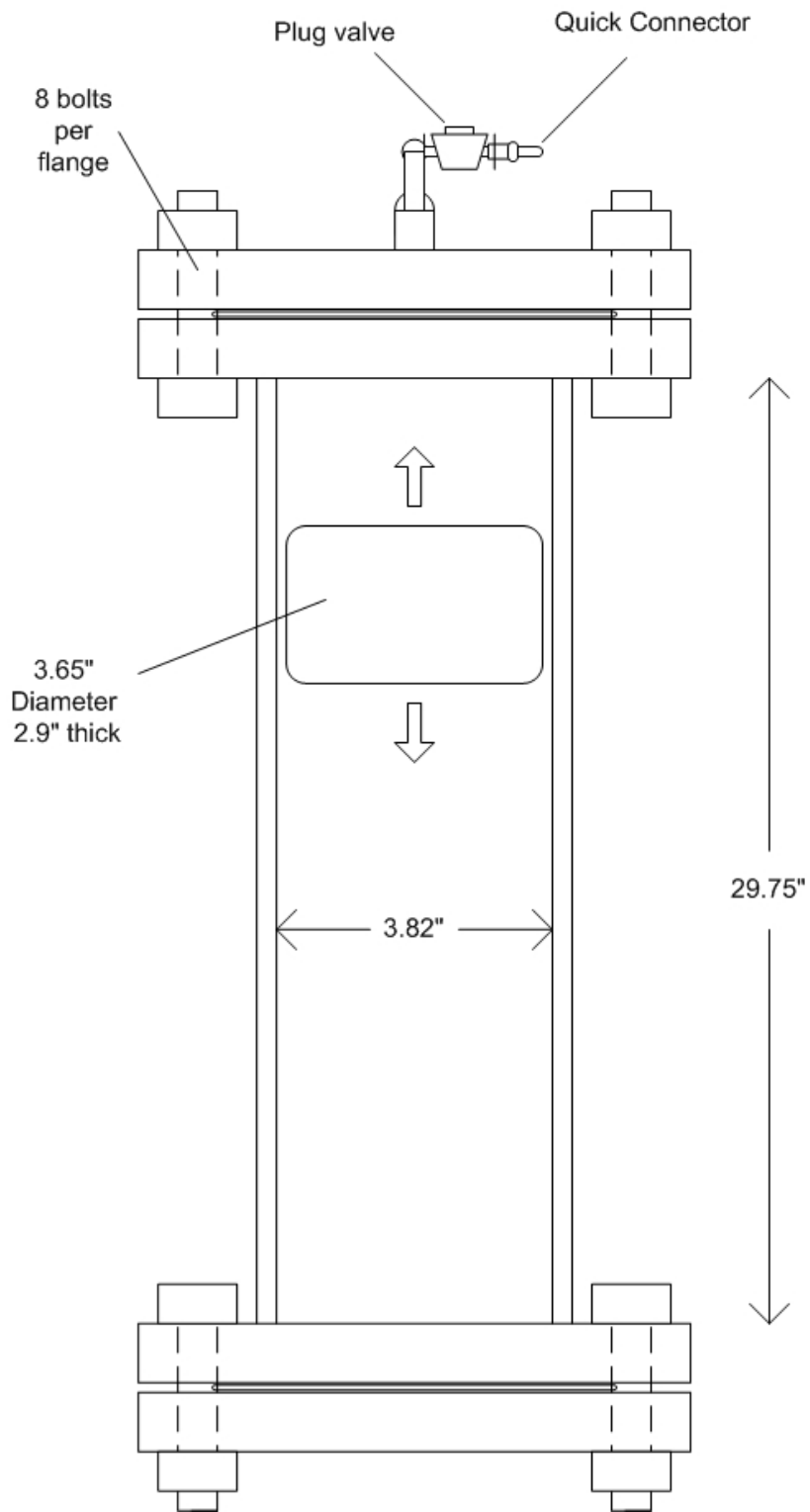


Fig. 4.10. Mixing vessel.

The mixing vessel is a stainless steel pipe (3.88 inch internal diameter and 29.75 inch internal length) with flanges (7/8" thick flanges, 8 bolts, and Buna-n gaskets) at both ends. The mixing element is a cylindrical Teflon<sup>®</sup> block (3.65 inch diameter, 2.9inch thick) mixing element. The volume of the mixing vessel is 4.9 L. Figure 4.10 is a schematic diagram of the mixing vessel.

The vessel is rotated lengthwise by a steel shaft (clamped on to the vessel), mounted with bearing blocks on top of the mixing stand. A DC motor coupled to the shaft rotates the mixing vessel. The motor is powered by a variable voltage controller, which enables rotation speed selection by voltage adjustment. The mixing vessel is connected to the gas loading manifold during the loading phase with a quick connect fitting and a flexible metal hose. The hose is disconnected from the mixing vessel while the mixing vessel is rotated during mixing. For each mixture, the vessel is rotated for 5 minutes, approximately 300 inversions. This is far greater than the 60 inversions required to achieve consistent combustion (10 out of 10 attempts) for a 3 % ethylene and 97 % air mixture.

The external mixer was selected to be the mixing method of choice after comparison with other methods. Internal mixing within the reaction vessel reduces the amount of flammable gases used per experiment, and it does not require loading the gas mixture to an external vessel before loading the gas mixture to the reaction vessel. For that reason two internal mixing methods were investigated before the external mixer was adopted. The first internal mixing method uses one to three brushless DC fans (Radioshack # 273-240, 12 VDC, 1.56 W) suspended from the top plate and one at the



bottom plate to produce turbulent regions within the reaction vessel where mixing will occur. The second method uses a bellows pump (1/4 horsepower, Baldor, model MB-111) to pull gas from the top of the reactor vessel and circulate it to the bottom of the vessel via a 1/8 in tubing while a brushless DC fan produces turbulence at the bottom of the vessel

The mixing methods were utilized with 3 % ethylene and 97 % air mixtures (within flammability limits according to previous works [2]) and tested for consistent combustion (10 out of 10 attempts). The first method of fan-induced turbulence was unable to mix the gas mixture sufficiently to obtain consistent combustion within a reasonable time frame (24 hours) even after increasing to three the number of fans at the top. The second method of pump-induced circulation was able to consistently mix the gas mixture sufficiently for combustion within 2 hours. These mixing methods were not used in this work because they require too much time to achieve reliable mixing.

#### 4.4 Sensors

Visual, pressure, and thermal sensors are used to detect combustion in this apparatus. The primary focus is on the behavior of the thermal measurements, using the visual and pressure measurements to confirm results.

The visual sensor is an Ultra Compact CCD camera (JPC-420P, 0.9 in × 0.9 in × 0.45 in, 0.01 lux, electronic shutter speed of 1/60 s) that outputs a black and white video stream. The camera is mounted on the bottom plate of the reaction vessel and directed

such that its field of vision captures the fuse wire explosions during ignition as well as light from a flame propagating away from the igniter. The video captured during an experiment clearly identify whether the fuse wire explodes or fails to explode, and whether the flame dies out or propagates after the fuse wire explosion.

The pressure within the reaction vessel is monitored with a dynamic pressure transducer (Omega DPX 101) mounted on the top plate. The piezoelectric quartz transducer has a range of 0 to 250 psig pressure rise, with 0 to 5 V nominal output signal, 1  $\mu$ s rise time, 1 % amplitude linearity, and temperature effect of 0.03 %/ $^{\circ}$ F. The pressure transducer is mounted on the 1/8 in NPT port on the top plate of the reaction vessel, sufficiently distant from the ignition source so that heat effects on the measured pressures are negligible. Maximum pressure is obtained by integrating the portion of the dynamic pressure vs. time curve that is above the baseline, and applying a conversion factor of 51.02 psi per V·s (from manufacturer specification).

The thermal sensors are five NTC thermistors (Thermometrics, 0.10 s response time in still air, 100 k $\Omega$  with 25 % variance, laboratory tested to be 107 k $\Omega$ ). NTC thermistors are thermal resistors with large negative temperature coefficients of resistance (resistance decreases as temperature increases). There are several major advantages to using thermistors instead of thermocouples or resistance temperature detectors (RTD). First of all, the thermistors have very small masses, and as a result they have very quick response times. Secondly, the high resistance of thermistors compared to the resistance of the wiring in the circuitry means the noise from those factors is negligible. Lastly, thermistors are very stable against high temperature, as well

as shock and vibration effects [30]. The first and third advantages are significant for measurements during combustion events where speed and stability are major considerations. For the purpose of this research, the main disadvantage of thermistors is that the resistance to temperature characteristic is only roughly linear over a relatively short range (0 to 80 °C for the thermistors used). However, the temperature trends can still be observed accurately with thermistor sensors.

The thermistors are suspended at the center axis of the reaction vessel at different lengths from the top by a frame consisting of two 1/8 in thick rods hanging from the top plate with short rods welded on at regular intervals for the signal wires to bundle around. The signal wires are AWG 26 enamel coated copper wires covered with Voltrex tubing insulation to prevent electrical shorts. They connect outside the reaction vessel by a pair of electrical feedthroughs constructed from 1/2 in diameter stainless steel sleeve around 1/4 in tubing sealed with epoxy (J-B Industro-Weld) and topped with silicone sealant to protect the wiring from damage. Figure 4.11 shows the thermistor positions. The signal wires are connected through shielded cables to the Wheatstone Bridge circuit to prevent interference from external electromagnetic sources (power lines, and other electrical devices in the lab).

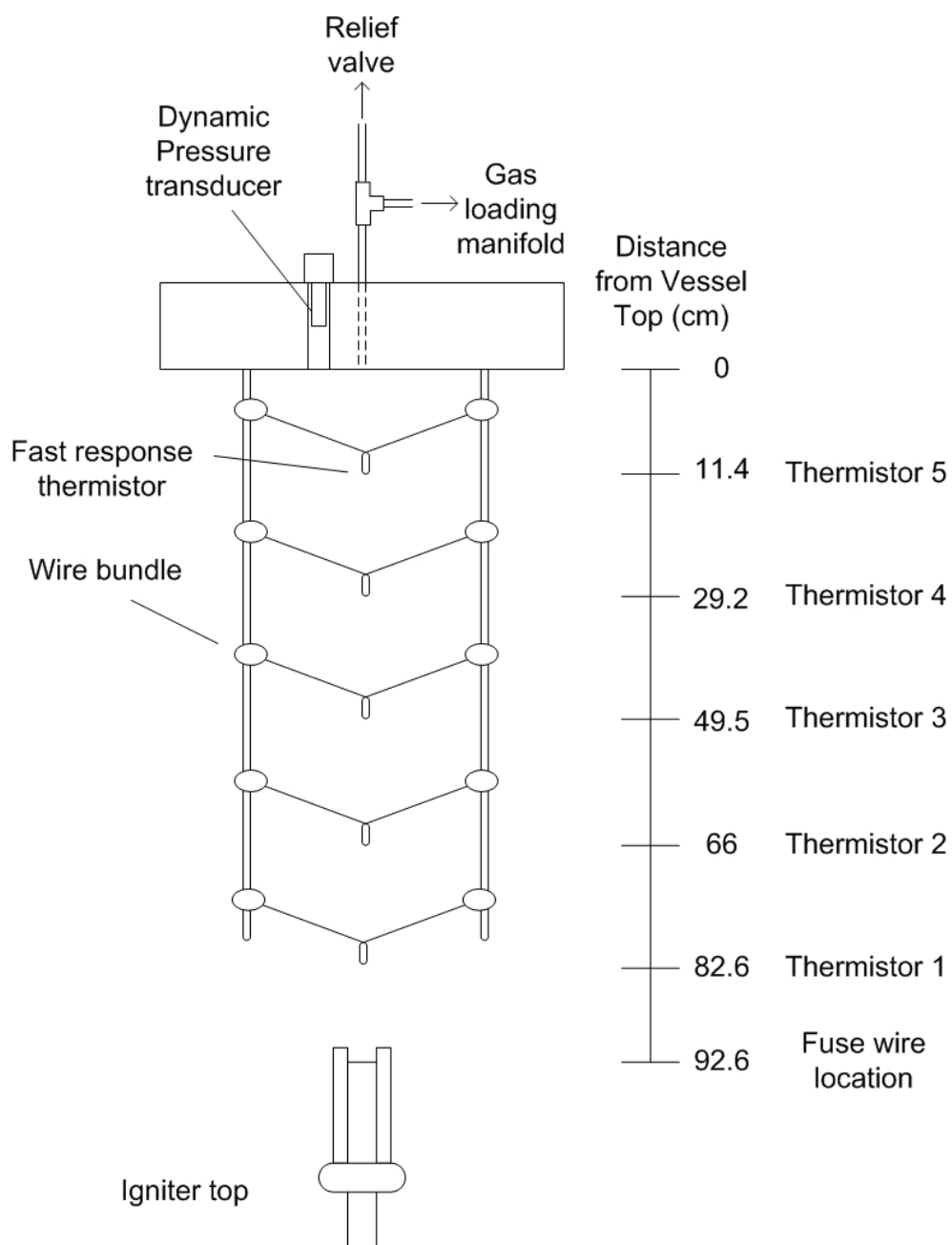


Fig. 4.11. Thermistor and fuse wire igniter positions relative to the reaction vessel top plate.

The Wheatstone bridge circuit consists of 4 resistor elements, one of which is the resistance to be measured, along with a constant voltage source and a voltage measurement device [31] as shown in figure 4.12.

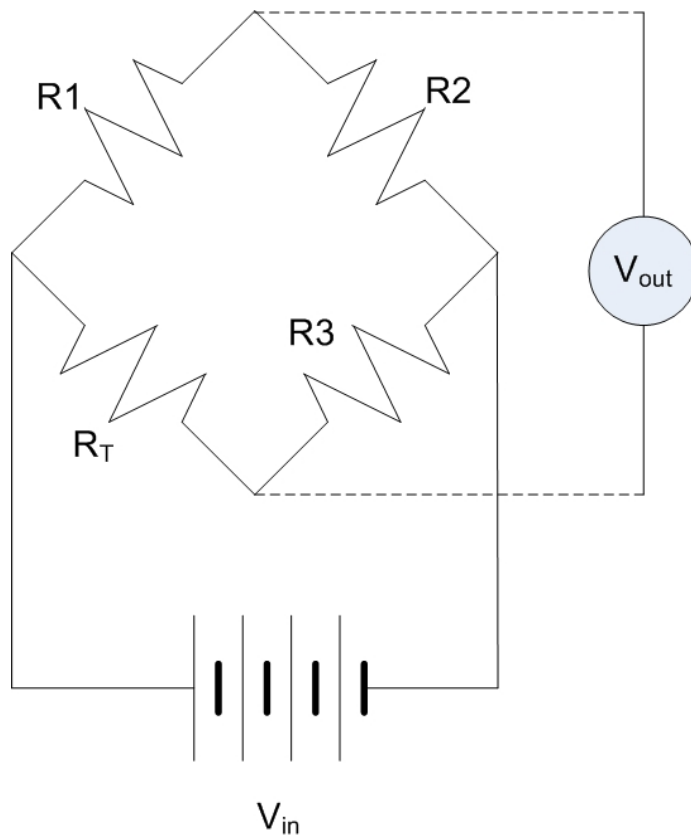


Fig. 4.12. Sample Wheatstone bridge circuit.

The advantage of this circuit is that, unlike resistance, the voltage difference can be measured directly and converted to resistance values as long as the values of the other three resistors are known. In the case where the bridge is initially balanced

(resistances adjusted so that  $V_{out}$  is 0) the change in the voltage output is roughly linear to the change in resistance for small resistance changes [31]. Figure 4.13 shows the thermistors' signal output from 10 to 260 °C as calculated from the Wheatstone bridge parameters and thermistor calibration information from the manufacturer.

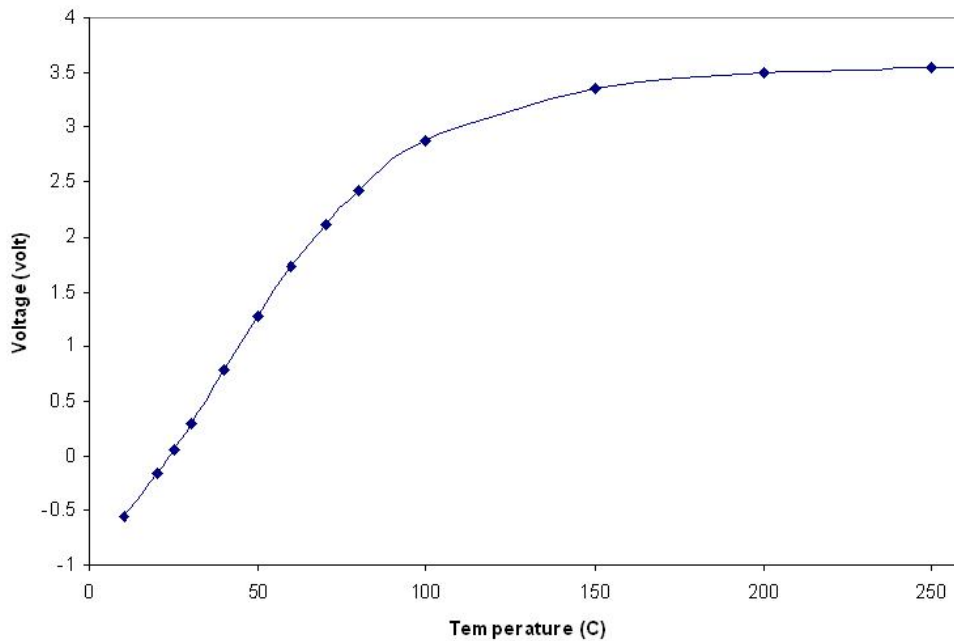


Fig. 4.13. Wheatstone bridge voltage as a function of thermistor temperature.

For the purpose of flame detection rather than flame temperature determination, calculation of the temperature is not necessary as passage of a flame will induce sharp increases in the voltage signal. Temperature trends of the gas mixture during and after combustion can be observed, providing data for qualitative analysis. The circuit used for

the flammability apparatus is actually five circuits with a common voltage source provided by the data acquisition device (details to be discussed later in this section).

Data acquisition is performed with a desktop computer (Dell<sup>®</sup> Optiplex 210L, with Windows XP<sup>®</sup>) equipped with a video capture device (Belkin<sup>®</sup> USB Videobus II), and a Keithley<sup>®</sup> data acquisition card (Keithley<sup>®</sup> KPCI-3102, 8 differential inputs with total of 225k signals per second @ 0.05 % accuracy) with screw terminal attachment (Keithley<sup>®</sup>, STP-68). The video stream from the camera inside the reaction vessel is processed by the video capture device and recorded with the MGI VideoWave IV SE<sup>®</sup> software in standard \*.avi format. The data acquisition card measures differential voltages, allowing it to measure both the thermistors and the pressure transducer. The measurement process is controlled by a Labview<sup>®</sup> (National Instruments, version 7.1) program.

#### 4.5 Igniter system

The ignition system for the apparatus has three design requirements. The first is the ability to ignite the gas mixture with a known amount of energy. Igniter energy is one of the parameters that can affect the flammability limit determined, and a consistent input of energy is required if the results are to be valid. The second is a consistent power delivery by the igniter. It is established that power density has a strong influence on the success of ignition, and review of past works showed that a high power density ( $> 1 \text{ MW/cm}^3$ ) allows gas ignitions with 1 to 100 mJ of energy, but when the power density is

low, the energy required to ignite gas mixtures is much higher than it would be otherwise [2]. If the power delivery has a varying pattern, even if the energy delivered is the same the results can be affected. The third is that the igniter system should require minimal efforts to operate. The ability to quickly and conveniently replace the fuse wire and reload the igniter is necessary for acceptable turnaround times between experiments.

The igniter system used in these experiments is similar to that outlined in ASTM E 918-83, which was demonstrated by Mashuga to be capable of inputting 10 J of energy with a repeatable power delivery [29]. The ignition source is a 10 mm piece of AWG 40 tinned copper wire, vaporized by a 500 VA isolation transformer (Hammond 171 E) at 115V AC switched on with a zero-crossing solid state relay (Omega, model #SSRL240DC100) so that the current is delivered beginning at the zero point of the AC cycle each time. Figure 4.14 shows the igniter system circuitry.

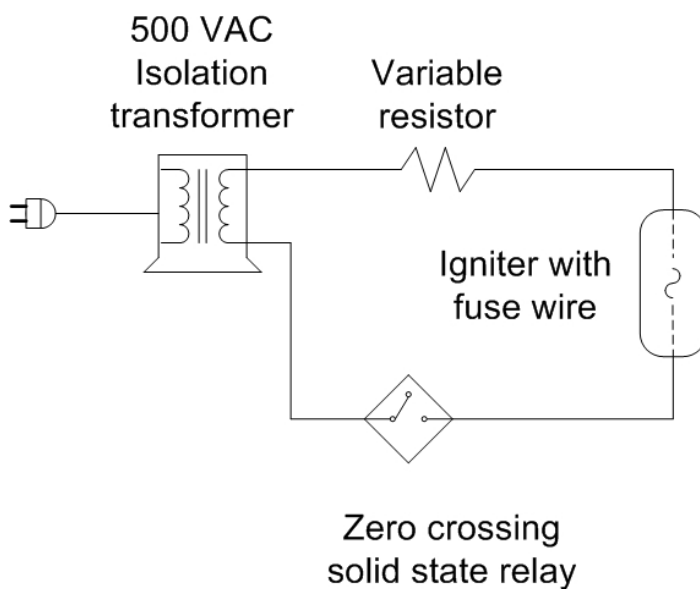


Fig. 4.14. Igniter system circuitry.



The igniter that holds the fuse wire consists of a wire holder section and a vessel seal section. The wire holder section is a pair of square copper rods with a spring loaded wire grip section mounted on a cylindrical platform made of non conducting polymer. The fuse wire is connected to the igniter circuit via the copper rods, which are soldered to wiring that leads outside the reaction vessel via the vessel seal section. The wire holder section is connected to the seal section with a short ¼ in stainless steel tube, which also contains the circuit wiring. The seal section is a Cajon<sup>®</sup> VCO O-ring face seal connector gland and screw cap. The center of the gland is fitted with a stainless steel plug and welded. The circuitry wiring is routed through a ¼ in hole in the plug, which is filled with epoxy to provide a hermetic seal. The igniter port on the bottom of the ignition vessel consists of a tapped 1 in NPT hole with the VCO face seal male connector portion (with Viton<sup>®</sup> O-ring) installed. The pressure seal is accomplished by inserting the igniter into the port and tightening the screw cap. Figure 4.15 shows the igniter design.

An alternate igniter system was considered, tested, and rejected prior to adopting the final design. Power delivery via a filled, large capacitor is very consistent, thus capable of fulfilling the requirements for the igniter circuitry. Figure 4.16 shows the circuit with a capacitor as ignition power source.

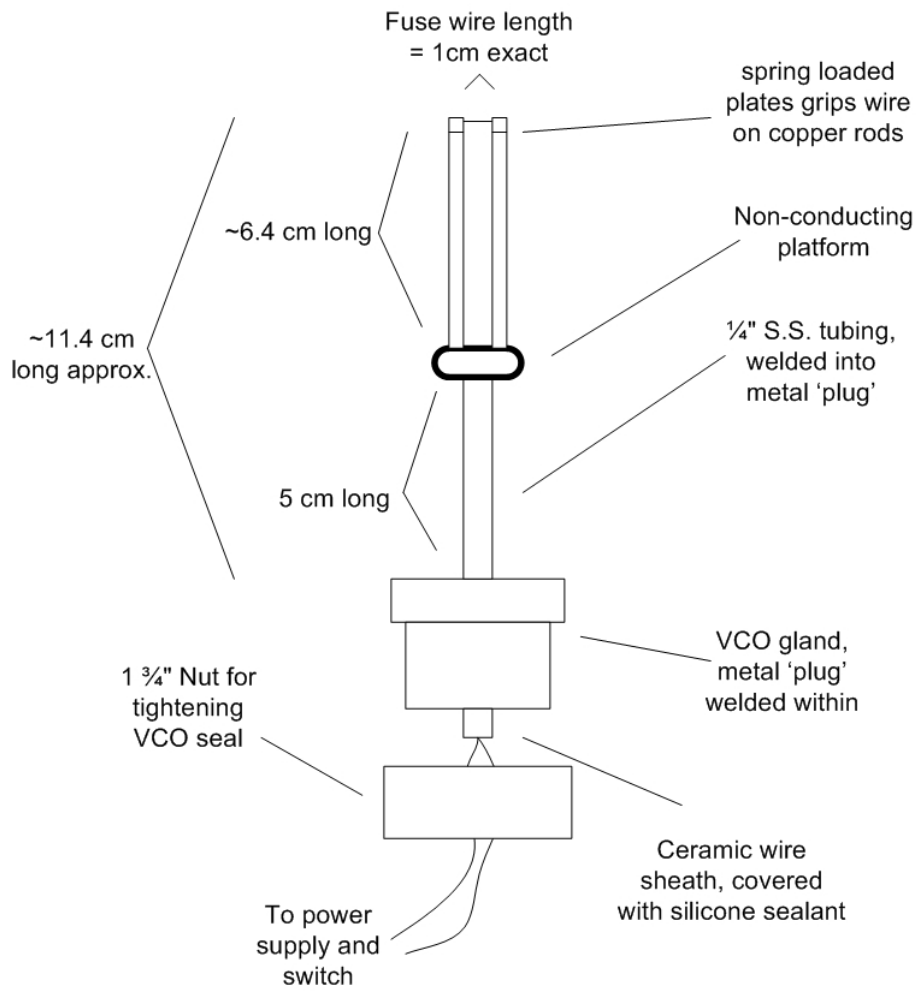


Fig. 4.15. Igniter.

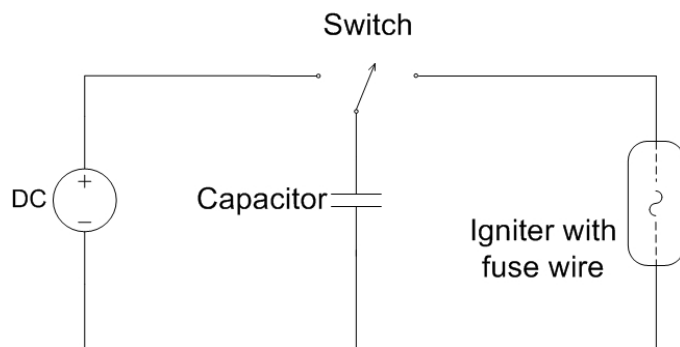


Fig. 4.16 Capacitor based igniter circuit.

Unfortunately capacitors of sufficient capacitance to supply adequate energy generally have a significantly lower voltage capability than that provided by the AC circuit. Experiments were conducted with a 24 Volt, 2 Farad Capacitor and 40 AWG tinned copper wire with ethylene air gas mixtures as well as methane air gas mixtures. As expected, the lower voltage input reduces the power density of the ignition source, rendering the ignition system adequate to start combustion. Multiple high voltage low capacitance capacitor can be linked to bypass this problem, but the equipment cost is significantly higher than the AC circuit so this alternative was rejected.

#### 4.6 Safety analysis

A full safety review was conducted during the design phase of this project, and repeated before each modification. A brief analysis of the final design of the flammability apparatus is presented here.

There are several potential hazards associated with the operation of the flammability apparatus. In order of consequence, the hazards are: 1) fire and explosion hazard from overpressure of the reaction vessel or manifold or mixing vessel, 2) fire and explosion hazard from leaked flammable gases, 3) electrical hazard from igniter system, and 4) physical hazard from moving or movable parts. The following discussion describes the hazards in more detail and the actions taken to reduce overall risk.

Analysis of the first hazard begins with understanding the potential pressures that the apparatus might experience. The flammability apparatus was used for flammability

limit determinations at atmospheric pressure (~1 bar). In the unlikely scenario where operational procedures were followed incorrectly, the gas mixture pressure within the reaction vessel can be higher, though not necessarily flammable (higher pressure might be due to incorrect loading of oxidizer or inert gas). According to observations by U.S. Bureau of Mines [9], combustion can occur as a deflagration or a detonation. During deflagration the flame velocity is less than the speed of sound, and the combustion can produce pressure waves roughly 8 times that of the starting pressure. During detonation the flame velocity exceeds speed of sound, and the combustion can produce a pressure wave roughly to 40 times the starting pressure [9]. A conservative estimate that the maximum pressure wave is 50 times that of planned initial pressure, either due to error in vessel loading or an unusually powerful detonation, yields a theoretical maximum pressure of approximately 50 bar. According to the Texas A&M chemical engineering department safety regulations, the apparatus must be designed to withstand at least 1.5 times the anticipated maximum pressure (~76 bar or 1100 psia).

The sections of the apparatus that are likely to experience pressure from the combustion are the reaction vessel and the gas loading manifold. The reaction vessel design took this into consideration, and was designed to fail at 103.4 bar or higher using modified guidelines from ASME design guide [32]. The reaction vessel has been tested hydrostatically to 82.74 bar, sufficient for the needs of the apparatus. In addition, two independent safety measures are in place, a relief valve and an enclosure around the reaction vessel. The relief valve at the top of the reaction vessel (Swagelok<sup>®</sup>, R4 Proportional Relief Valve) relieves directly into the laboratory vent at 500 psig or

higher, which mitigates the pressure damage without releasing flames or hot gases into the laboratory. The vessel enclosure provides two functions. The enclosure walls (1/8 in thick steel or double layers of 1/4 in thick Lexan<sup>®</sup>) offer protection from shrapnel in extreme cases where the vessel is unable to withstand pressure produced during combustion. It also supports the apparatus at a sufficient height such that disassembly of the reaction vessel can be accomplished with the lowering of the reactor body rather than lifting, thus reducing safety hazards of reactor body weight during maintenance and modification.

The gas loading manifold is usually blocked from the reaction vessel with a closed stainless steel plug valve (Swagelok<sup>®</sup>, or Cajon<sup>®</sup>) with a pressure rating of 3000 psig. In the case where the valve is left open by operator error, the components in the manifold may experience high pressure. The 1/4 in tubing, the plug valves, and the metering valve in the manifold are all stainless steel with Swagelok<sup>®</sup> compression fittings and working pressure ratings of 2000 psig or higher. Since the pressure ratings of components in the manifold are greater than the expected maximum pressure, the hazard from higher than normal operating pressures in the manifold components is negligible.

The mixing vessel usually contains higher than atmospheric pressure gas mixtures (~23 psig) during loading and mixing. However, it does not present a hazard from combustion because the only internal wetted components are a Teflon<sup>®</sup> block and the stainless steel vessel walls, neither of which can provide an ignition source. Combustion can not occur without an ignition source

The hazard of gas leaking from the apparatus is also negligible. First, all gas cylinders are stored in a vented corridor separate from the laboratory space, with pressure regulators attached directly to the storage cylinders. Fuel gases are fed to the apparatus at lower than atmospheric pressure, thus flammable gas leaking out of the apparatus only can occur after loading of oxidizer or inert gas. Any flammables leaking out of the apparatus would be at a low concentration, and very small in volume relative to the laboratory. The laboratory is exhausted constantly, making the occurrence of a flammable gas mixture in the laboratory highly unlikely.

Electrical hazard from contact with exposed circuitry is also negligible. All reachable exposed portions of the circuit are covered with either silicone sealant or electrical tape.

Physical hazard from moving parts comes in two forms: the reaction vessel body during maintenance, and the mixing vessel during gas mixing. The first hazard is rendered negligible by counter balancing the reaction vessel weight with a counterweight-pulley system, preventing damage to equipment or operator because the vessel body cannot drop suddenly. The mixing vessel rotation can cause harm to the operator through impact, and damage to the gas loading manifold if it is still connected to the manifold when motor is turned on. A spring-based coupling sheath is installed connecting the motor shaft to the mixing vessel shaft. The mixing vessel is decoupled from the motor if a relatively small amount of force is applied to it in the opposite direction of the rotation. This effectively forces the rotation to be started slowly during

experiments to avoid decoupling, but mitigates any impact it might have on the operator and equipment.

## 5. METHODS AND PROCEDURES

### 5.1 Overview

The flammability apparatus operation consists of several steps: evacuate the vessels and connecting lines; load the gases into the mixing vessel; evacuate the manifold between loadings; mix the gases; load the gas mixture into the reaction vessel; ignition and data acquisition; and preparation for the next experiment. Detailed procedures for these steps are provided to minimize error in the gas mixture compositions and to reduce risk from safety hazards caused by operator error. In addition, several maintenance and preparatory procedures are required before each experiment.

### 5.2 Apparatus setup

Setup of the flammability apparatus consists of leak tests, gas regulator checks, sensor tests, and cleaning. Leak tests are performed after every vessel cleaning, modification, or extended period of dormancy. This involves evacuating the reaction vessel, manifold, and mixing vessel to a moisture-free state, then observing the pressure after thermal equilibrium is established. The pressure is recorded for 4 hours and the leak rate determined. For several tests, the leak rate was found to be 0.015 psia/hr. If the



leak rate is greater than this the reaction vessel and mixing vessel flange bolts should be retightened.

The apparatus uses pressurized cylinders to supply gases during loading. The pressure of the incoming gas is determined by the setting of the pressure regulators on each cylinder. Fuel cylinders should be adjusted to -6 psig, whereas oxygen or air should be 30 psig and inerts 40 psig. The numbers are arbitrary, but the pressures selected ensure precision during gas loading and that very little fuel gas can leak out of the gas line if the manifold accidentally is opened to the laboratory.



Fig. 5.1. Video capture software control panel.

Sensor tests are performed each day before experiments are begun. The video sensor is checked by examining the video output in the video capture software. Figure 5.1 shows the control panel of the MGI VideoWave<sup>®</sup> software. The pressure and thermal sensors are checked by observing the graphical output from the Labview<sup>®</sup> panel and ensuring that the range and noise level of the readings are within normal parameters. Figure 5.2 shows the Labview software panel during a test.

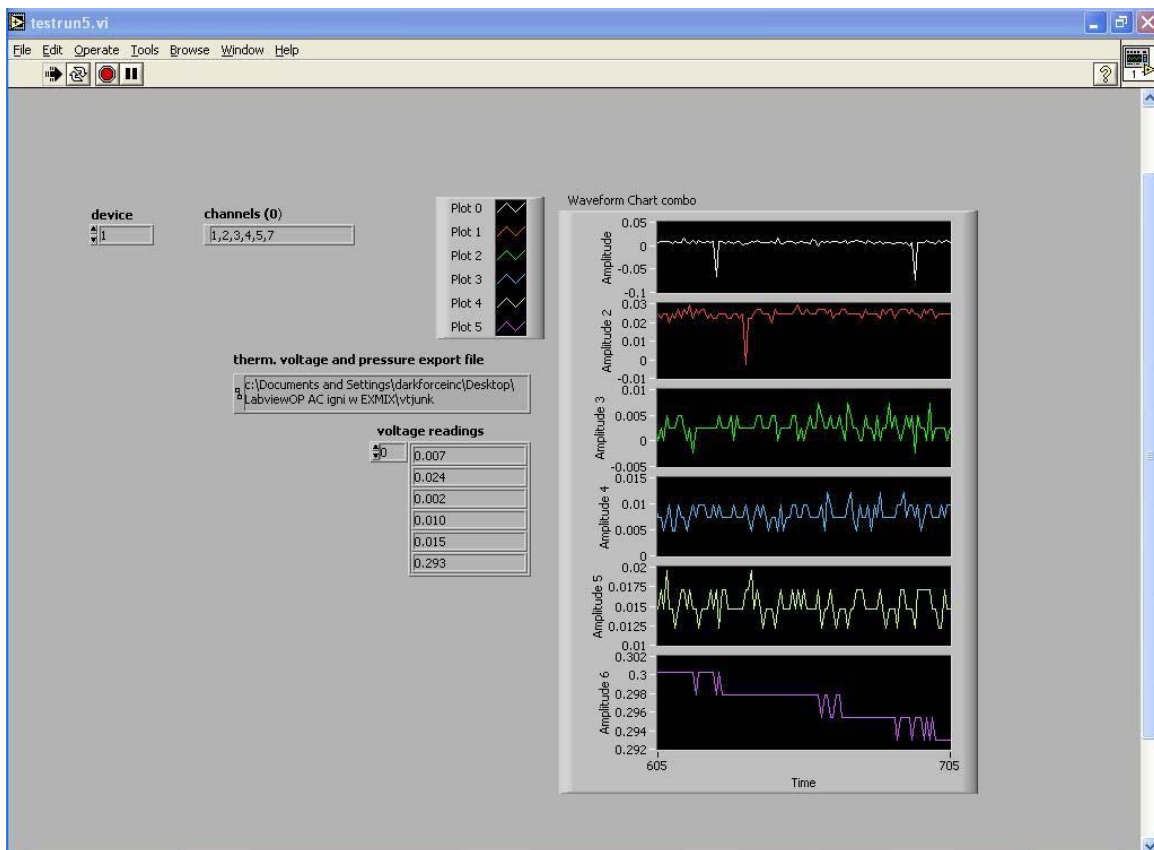


Fig. 5.2. Labview control panel for pressure and temperature readings showing voltage (in V) as a function of time (in ms).

Soot deposits on the reaction vessel and the igniter can result from incomplete combustion. The soot can introduce error into the gas mixture concentrations through adsorption and or absorption of components, and also reduce the contact between fuse wire and igniter. The vacuum pump oil also can be contaminated, reducing the pump efficiency. Every 100 experiments, the reaction vessel is cleaned with ethanol and acetone, and the oil of the vacuum pump is replaced. The igniter is cleaned with a toothbrush to remove majority of the soot, and also fuse wire fragments that remain in the fuse wire grip. The contact surface at the fuse wire grip also is smoothed with fine sand paper occasionally to remove melted copper drops.

### 5.3 Operating procedure

Step 1: Preparation for gas loading consists of evacuating the reaction vessel, mixing vessel, and the gas loading manifold. Figure 5.3 shows the configuration (opened/closed state) of each valve for this step. After the valves are in the correct positions, the vacuum pump is activated and allowed to run until the pressure is constant (pressure change no greater than 0.01 psi) for over one minute. The pump is then deactivated, and the pressure is recorded for gas mixture composition calculations on an Excel spreadsheet.

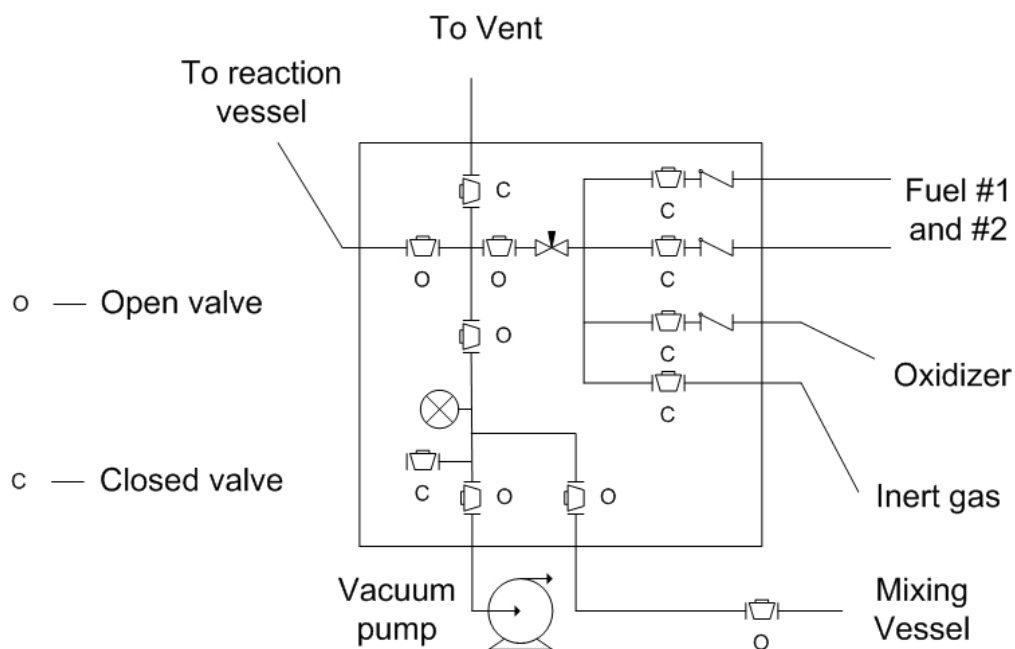


Fig. 5.3 Valve configuration for evacuating the mixing vessel, reaction vessel, and manifold.

Step 2: The mixing vessel is filled one gas at a time. The fuel is the first gas to be loaded through the manifold into the mixing vessel. Figure 5.4 shows the configuration of each valve for this step. The fuel is loaded into the mixing vessel until a predetermined pressure is reached, using the metering valve to achieve precise pressure control. The final pressure is recorded on an Excel spreadsheet to calculate the gas mixture composition.

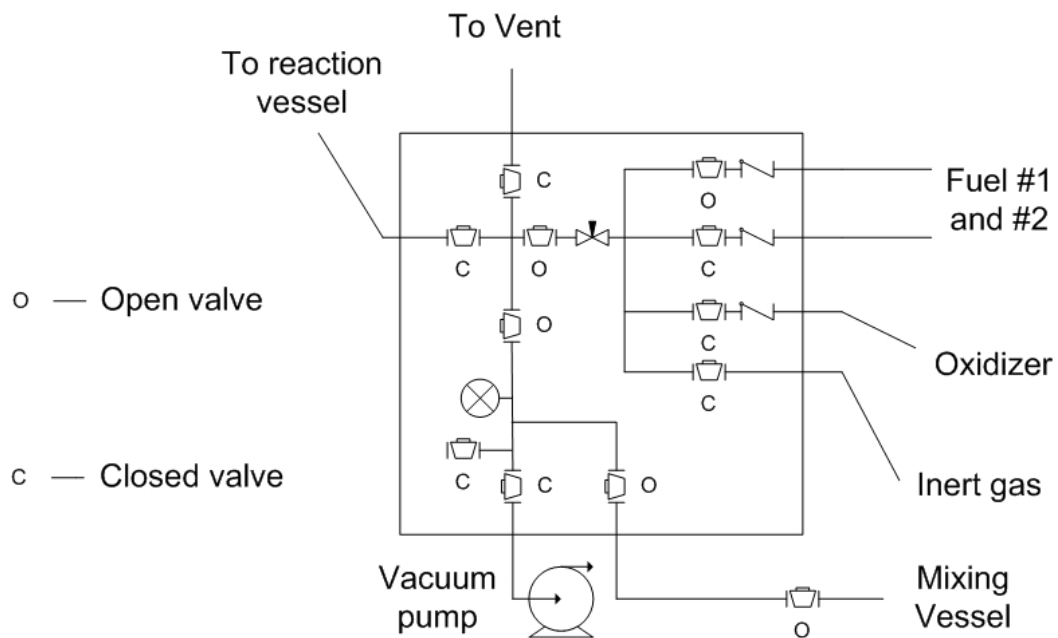


Fig. 5.4 Valve configuration for loading fuel #1 into the mixing vessel.

Step3: The gas loading manifold is evacuated between each gas loading. Once the valves are configured as shown in figure 5.5, the pump is activated until the manifold pressure is constant (pressure change no greater than 0.01 psi) for 10 s.

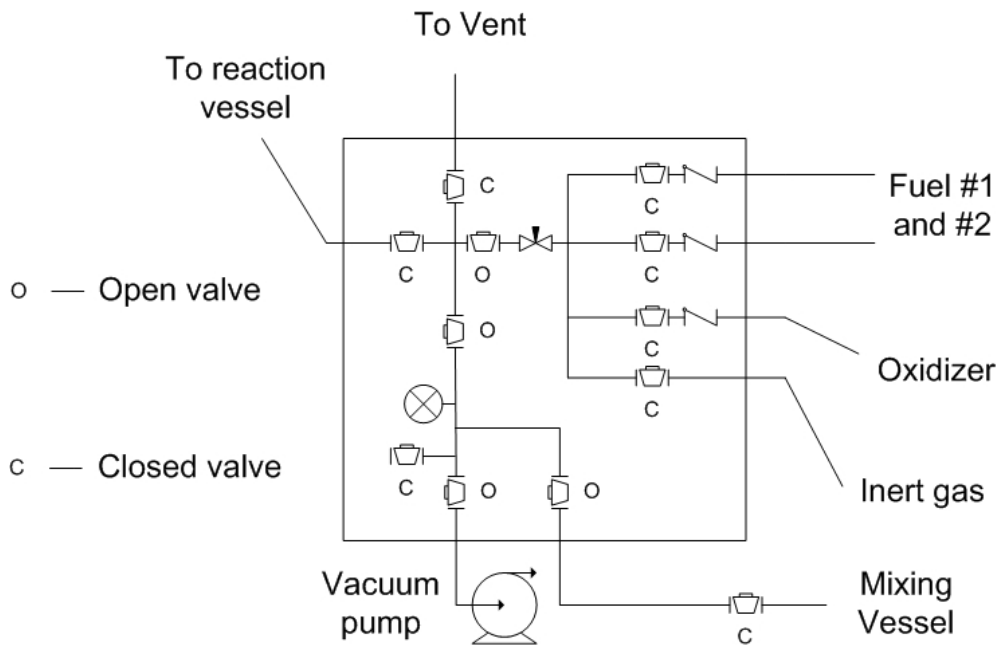


Fig. 5.5 Valve configuration for manifold evacuation.

Steps 2 and 3 are repeated as often as necessary to load all fuel, oxidizer and inert components required to create the gas mixture. Step 2 will vary slightly each time in that a different valve at the gas feed lines will be opened depending on the component to be added into the mixing vessel. The valve between the manifold and the mixing vessel should be the last valve to be opened for that step, to prevent gas flowing back into the manifold before gas loading.

Step 4: The external mixer is utilized after the gas loading is complete. Care should be taken to ensure that the plug valve on top of the mixing vessel is closed, the manifold opened to the ventilation, and then disconnect the mixing vessel from the manifold. After disconnection, activate the DC motor with slowly increasing voltage to the pre-set value (enables 30 rotations, or 60 inversions a minute) to start rotation. The

motor is de-activated after 5 minutes, and the vessel rotated backwards (making use of the safety feature of the motor to shaft coupling sheath) until the mixing vessel's top is in position, and reconnect to the manifold. Repeat step 3 again to clear the manifold.

Step 5: The gas mixture is loaded into the reaction vessel. Figure 5.6 shows the valve configuration for this step. The mixing vessel valve should be the last to be opened; after all other valves are opened or closed. Once the reaction vessel has filled to 14.7 psia, it should be isolated from the gas loading manifold by closing the valve between them. The inert valve then should be opened to lower the fuel concentration in the manifold and the mixing vessel until it is no longer flammable.

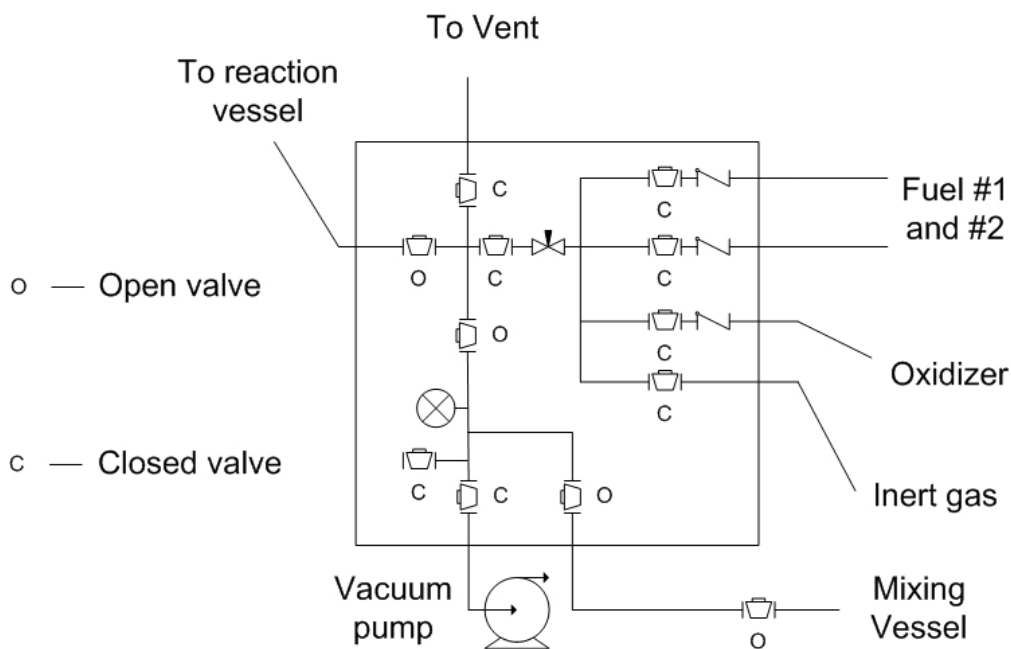


Fig. 5.6. Valve configuration for loading the test mixture into the reaction vessel.

Step 6: The ignition and data acquisition step is the most complex step, but still fairly simple. The gas mixture is allowed to sit in the reaction vessel for five minutes to reach thermal equilibrium and become quiescent. The Labview and MGI VideoWave software are activated to begin recording. Approximately 2 s after the data acquisition starts, a 5 V signal to the solid state relay activates it, which completes the igniter circuit at the next zero point of the AC power cycle. The ignition and the subsequent combustion (or lack of) can be viewed in real time through video or detected by the thermistor/pressure transducer readings. The video recording must be terminated manually, producing 7 to 10 s long \*.avi files. The pressure and thermistor readings stop automatically after 10 s, and are written into a data file in column format for easy importation into Excel. The readings are voltage values, with 2000 data points for each sensor (5 thermistors, 1 pressure transducer). This number of measurements is far lower than the maximum capability of the data acquisition card. However, the computer is not always reliable when acquiring voltage data at high speeds along with video capture, so a slower acquisition speed, which still provides adequate resolution, is used. The video file and the data files are named identically (with different file extensions), and the name recorded along with the combustion results.

Step 7: Preparing the flammability apparatus for the next experiment involves two tasks. The first task is to vent the reaction vessel. In the case where combustion occurred or the fuel concentration is below the lower flammability limit, the reaction vessel simply should be connected to the gas manifold and allowed to vent by opening the vent valve and the valve between reaction vessel and manifold. The next task is to



remove the igniter from the reaction vessel, clean it, replace the fuse wire, and reload it into the reaction vessel, taking care to tighten the screw cap to ensure pressure seal. This step normally requires 3 to 5 minutes.

In rare cases the ignition fails due to fuse wire damage. Accidental damage to the fuse wire resulting from handling or a defect in manufacturing can cause only a portion of the fuse wire to melt rather than for the entire wire to explode as required for consistent ignition. Since only a fraction of the 10 J ignition energy is delivered to the gas mixture, even a flammable mixture might not ignite. This situation can be detected by observing the video capture of the ignition event. In such a case, inert gas is loaded into the reaction vessel until the fuel concentration is well below the flammability limit (50 % or less) before venting. The flammability apparatus is ready for another experiment after completing these tasks. This procedure also should be followed when combustion does not occur because the gas in the vessel is above its upper flammability limit.

#### 5.4 Flammability limit selection method

The step size (step change made in the fuel concentration between experiments) and the number of repeat experiments are significant factors in the accuracy of the flammability limits determined. When a relatively small step size is chosen, the number of experimental repetitions must be increased to maintain accuracy.

Measurements of the flammability limits with the experimental apparatus uses 0.01 mol % step size for pure fuel in air and 0.02 mol % for all other experiments. These small step sizes are chosen because precise flammability values can be used more effectively in models and for comparisons with existing data of similar precision. Up to 10 repetitive tests are conducted per step to compensate for the small step size.

Common practice with American researchers, and recommended by ASTM methods [23], is to determine the lower flammability limit by averaging the lowest fuel concentration with flame propagation and the highest concentration in which flame will not propagate, *vice versa* for the upper flammability limit. This experimental definition is not directly applicable to repetitive experiments, since gas mixtures near the limit may or may not propagate after ignition. Wierzba *et al.* [15] showed that probability of flame propagation can vary from 0 to 100 % when the fuel concentration is within 1 to 2 % (relative) of the upper limit (defined by Weirzba as the 0 % propagation concentration). This demonstrates that flame propagation near the limits has a probabilistic nature.

It is expected that repetitive tests at the flammability limit will result in flame propagations in 50 % of the experiments because random parameter differences will distribute the mixture concentration above and below the flammability limit equally. Because the fuel concentrations tested are unlikely to be exactly at the flammability limit, there will be a pair of concentration values differing by one experimental step size where one is above and other below the limit. The experimental flame propagation rates for those fuel concentrations above and below the LFL and will be greater than 50 % and less than 50 % respectively and *vice versa* for the UFL. This research selects the fuel

concentration that is measured to have less than 50 % (4 or less flame propagations out of 10) as the flammability limit, unless the rate is 0 %, in that case the other concentration is selected as the limit.

## 6. RESULTS AND DISCUSSION

### 6.1 Overview

The flammability limits of hydrocarbons fuels, fuel mixtures in air, fuel mixtures in varying oxygen concentration, and minimum oxygen concentrations for hydrocarbon gases and their mixtures were determined using the thermal criterion developed for this apparatus. The experimentally determined flammability limits and minimum oxygen concentrations are compared with measurements reported in the literature. The mixture lower flammability limits are used to evaluate the Le Chatelier model applied to methane-propane and methane-butane mixtures in air.

Initial experiments with methane-air and ethylene-air mixtures were used to evaluate mixing and ignition configurations. These experiments utilized thermistor sensors in combination with video and pressure data to identify four types of combustion behavior in the flammability apparatus: non-propagation, flash, discontinuous flame propagation, and continuous flame propagation. A thermal criterion is developed for the flammability apparatus by matching combustion behavior with the signal *vs.* time curves of the thermistors.

## 6.2 Combustion types in reaction vessel

Combustion behavior observed in the flammability apparatus can be grouped in the following categories:

Non-propagation refers to the lack of flame propagation from the ignition source.

Flash combustion is a flame with vertical flame propagation, but little or no horizontal propagation, that terminates within a short distance of the ignition source to produce minor temperature and pressure increase.

Discontinuous flame propagation is a flame that propagates vertically and horizontally, but terminates before it reaches the top of the reaction vessel.

Continuous flame propagation occurs when the flame is able to propagate vertically and horizontally and does not terminate until it reaches the top of the reaction vessel.

The combustion behavior within the apparatus first was observed with experiments of methane/air and ethylene/air mixtures over a range of concentrations that span from above to below the lower flammability limits for these gases. The data from the video, pressure, and thermal sensors are acquired simultaneously, and interpreted to identify the combustion types. The video data is examined first due to ease of interpretation. The images made from frames captured from the videos are presented along with temperature and pressure data to facilitate identification of combustion type and thermistor signal *vs.* time curves in different combustion zones.

Non-propagation combustion is defined by the lack of flame propagation after ignition, which can be due to a variety of factors, such as very low fuel or oxidizer concentration, as well as low ignition energy or power. A blank experiment was conducted with air only (no fuel) at 14.7 psia to provide information about background effects.



Fig. 6.1. Images of non-propagation combustion in blank(air) experiment.

Figure 6.1 shows glowing droplets of fuse wire illuminating the interior of the reaction vessel for a short time period after the fuse wire explosion (ignition).

Illumination by fuse wire droplets lasted approximately 0.1 s. Images in figure 6.1 (and all subsequent figures with video captured images) are arranged in chronological order from left to right, top row to bottom row.

Figure 6.2 shows the temperature and pressure data. Non-propagation type behavior in the flammability apparatus has negligible pressure fluctuation (a single measurement that suggests a pressure pulse of 0.005 psi lasting approximately 5 ms), and a minor temperature increase at the lowest thermistor, approximately 10 cm from the ignition source. Note that the thermistors are numbered in an ascending manner, such that thermistor 1 is at the bottom and thermistor 5 is at the top.

The small temperature spike came from a portion of the gas heated by the ignition energy and rising to the lowest thermistor's area. The temperature quickly cooled because of heat transfer to surroundings, thus no change in temperature is indicated by the thermistors farther from the ignition source. The pressure and temperature data show that ignition energy from the igniter has negligible direct impact on the measurements during combustion.

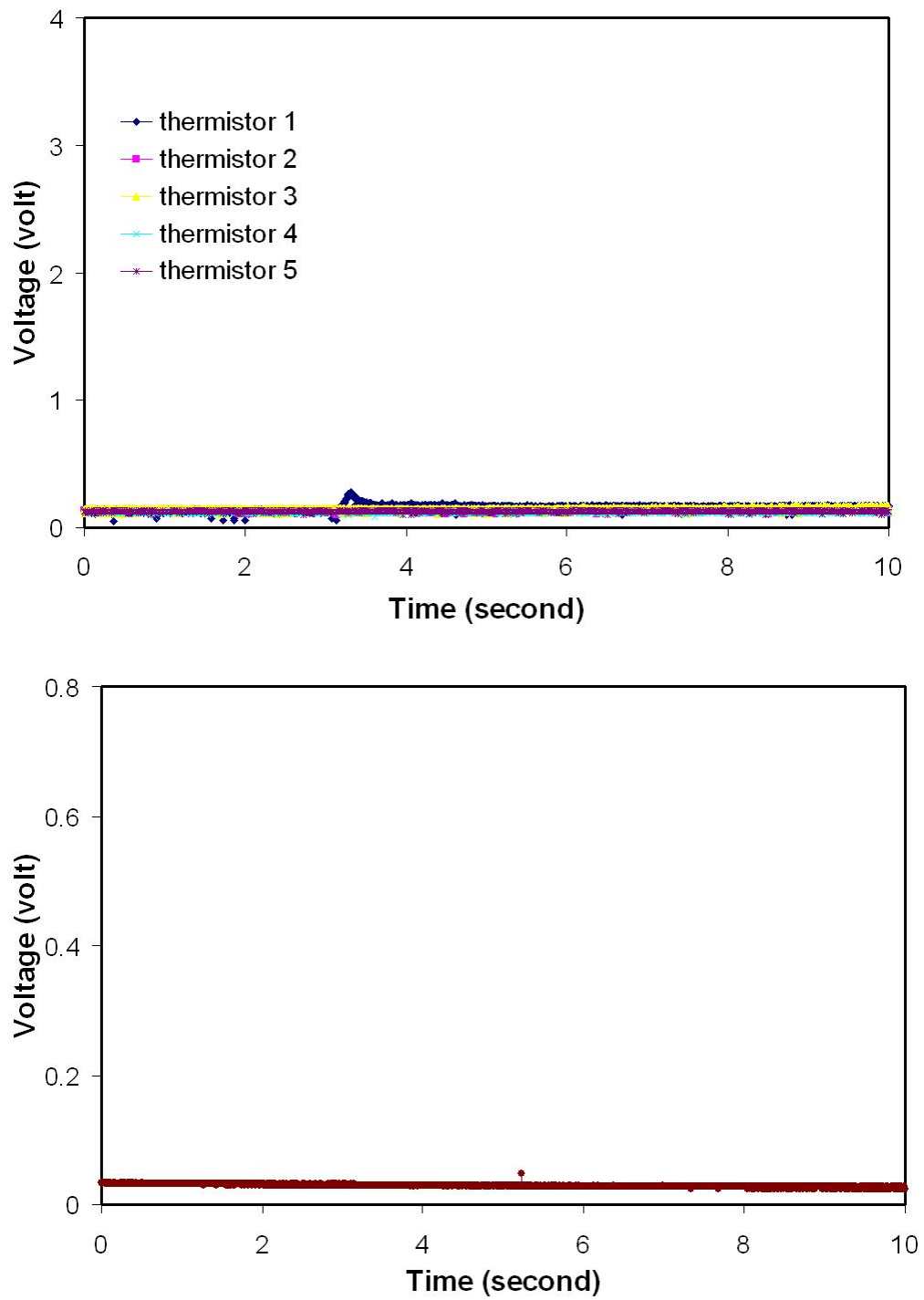


Fig. 6.2. Temperature (top) and pressure (bottom) profiles for non-propagation combustion.



The flash type combustion is a vertical propagation (little to no horizontal) of flame that terminates after a short distance from the ignition source. Figure 6.3 shows the images from igniting 4.26 % methane in air at 14.7 psia.

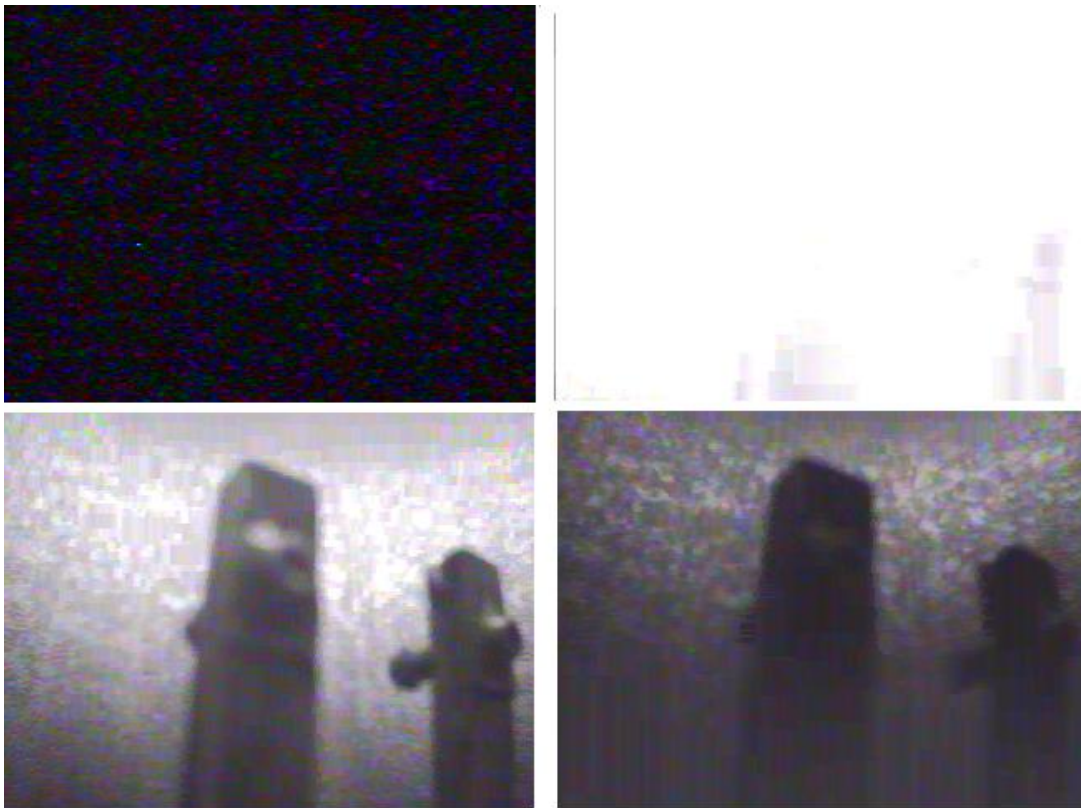


Fig. 6.3. Images of flash combustion. (4.26 % methane in air)



Fig. 6.3. Continued.

The images show combustion of the gas mixture surrounding the ignition source, and a rising source of illumination for a short period of time. The time between ignition and the end of the illumination is approximately 0.2 s, twice as long as the illumination provided by the fuse wire droplets. The increased time interval and the rising light source shown in figure 6.3 show that some of the gas mixture continued to burn above the ignition source after ignition. The video does not provide sufficient detail to determine the flame speed or the propagation distance of the flame plume.

Figure 6.4 shows the temperature and pressure data for flash combustion of 4.26 % methane in air at 14.7 psia.

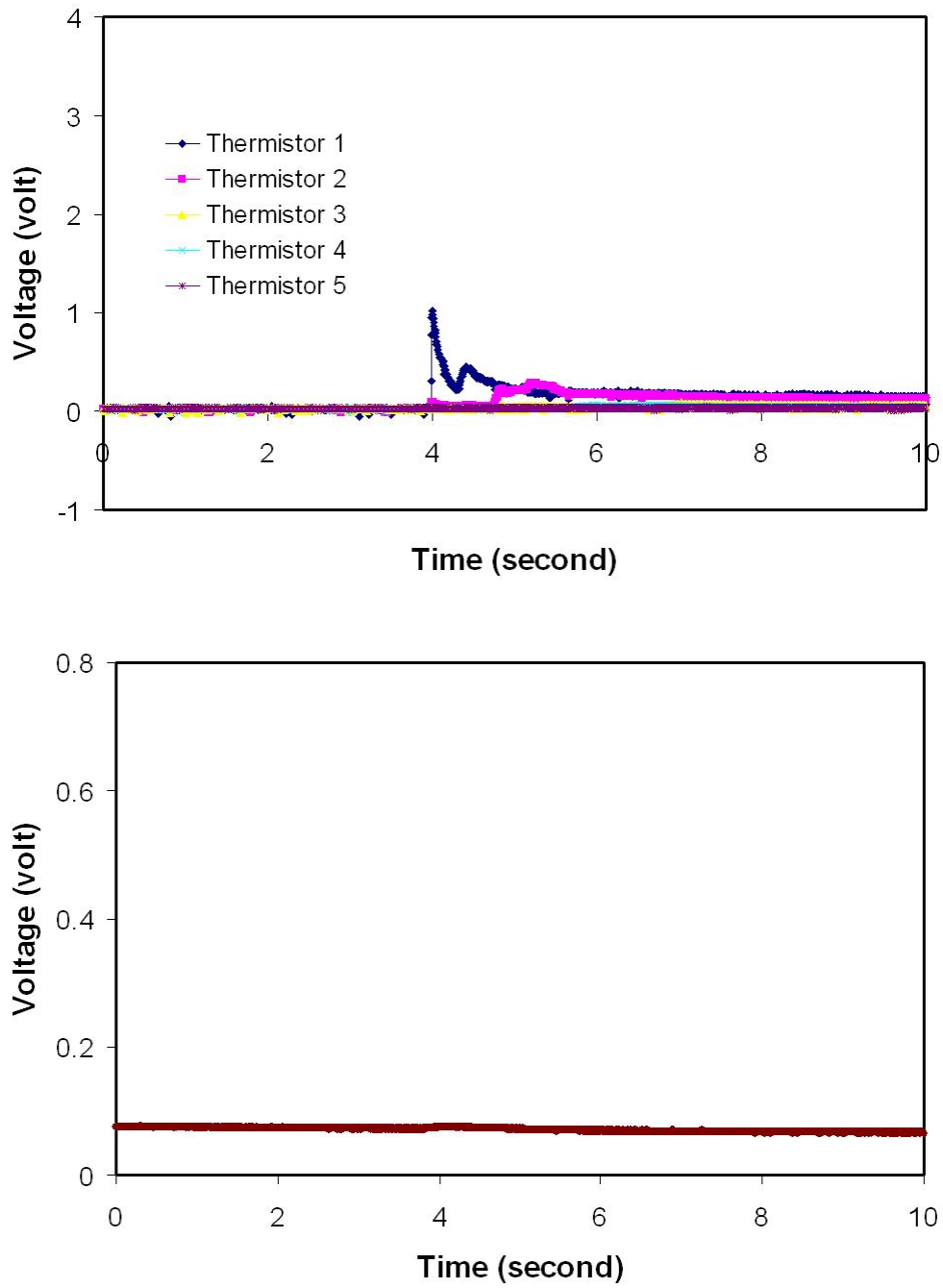


Fig. 6.4. Temperature (top) and pressure (bottom) profiles for flash combustion

The pressure measurements show a maximum increase of 0.20 psi (1.4 %). The large noise to signal ratio for the pressure data indicate a significant amount of relative error in the maximum pressure found, but it is clear that there is a small pressure effect caused by combustion of some of the fuel mixture. The temperature measurements show a temperature peak at thermistor 1 (peak temperature approximately 45 °C) and a minor temperature increase at thermistor 2.

The flash combustion example shown here has a very minor temperature and pressure increase, but some flash combustions have greater temperature and pressure increases. In some cases, the signal from thermistor 2 also exhibits a peak, indicating that the flame plume propagated sufficiently to affect the temperature there.

Discontinuous flame propagation is a flame that propagates vertically and horizontally, but terminates before reaching the top of the vessel. Figure 6.5 shows the images from igniting 5.00 % methane in air at 14.7 psia. The images show the fuse wire explosion igniting the gas in its surrounding, and the flame plume propagates upward away from the ignition source. Within a short time a wider flame propagates back down, demonstrating downward and horizontal propagation. Downward and propagation past the initial flame path indicates the presence of uncombusted gas. This shows that the flame plume is initially relatively narrow compared to the vessel width, allowing a sizable volume of gas to avoid combustion on the first pass of the flame.

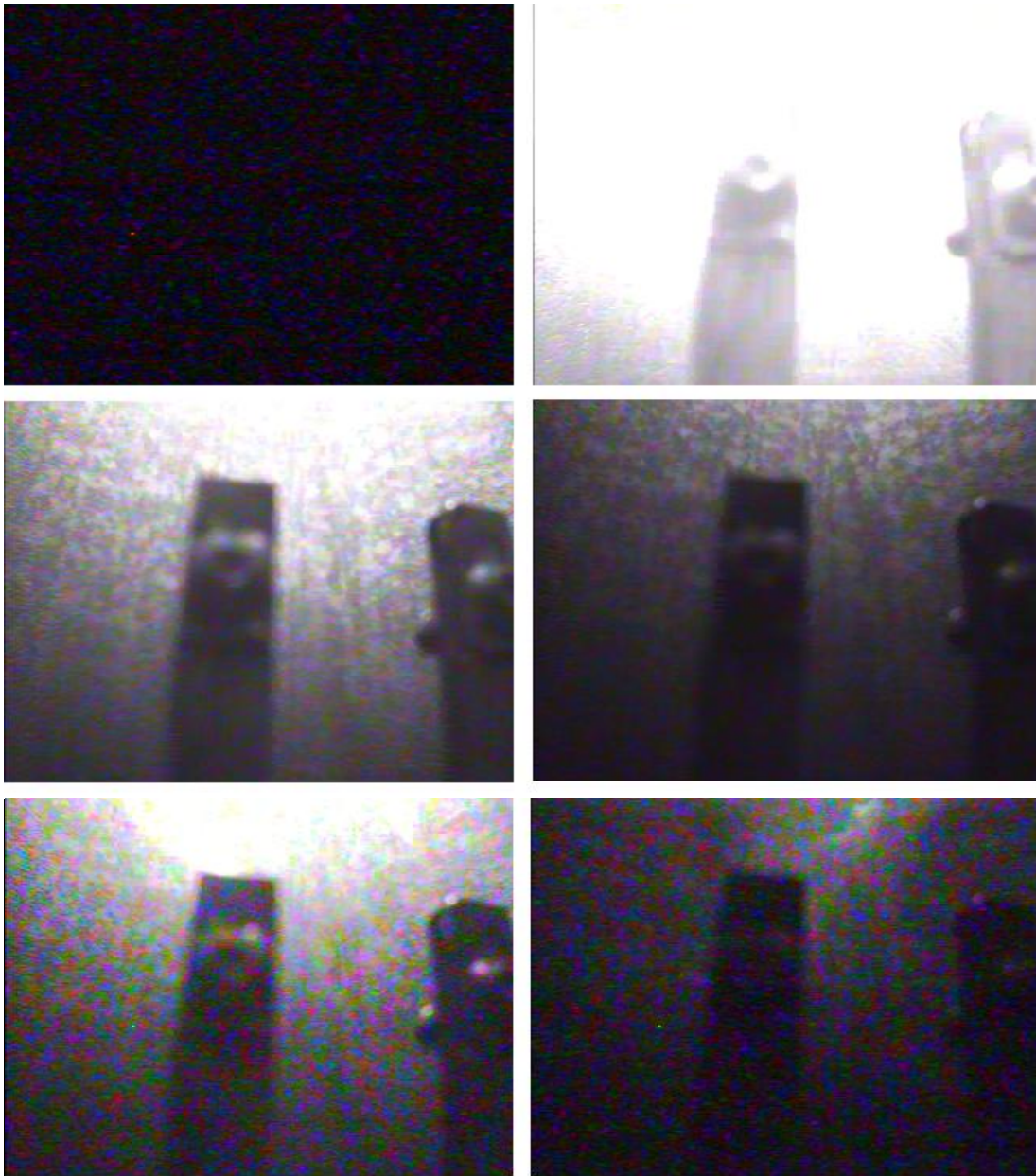


Fig. 6.5. Images from discontinuous flame propagation. (5.00 % methane in air)

The temperature and pressure profiles of discontinuous flame propagation differ substantially from the profiles of flash combustion (see figure 6.6).

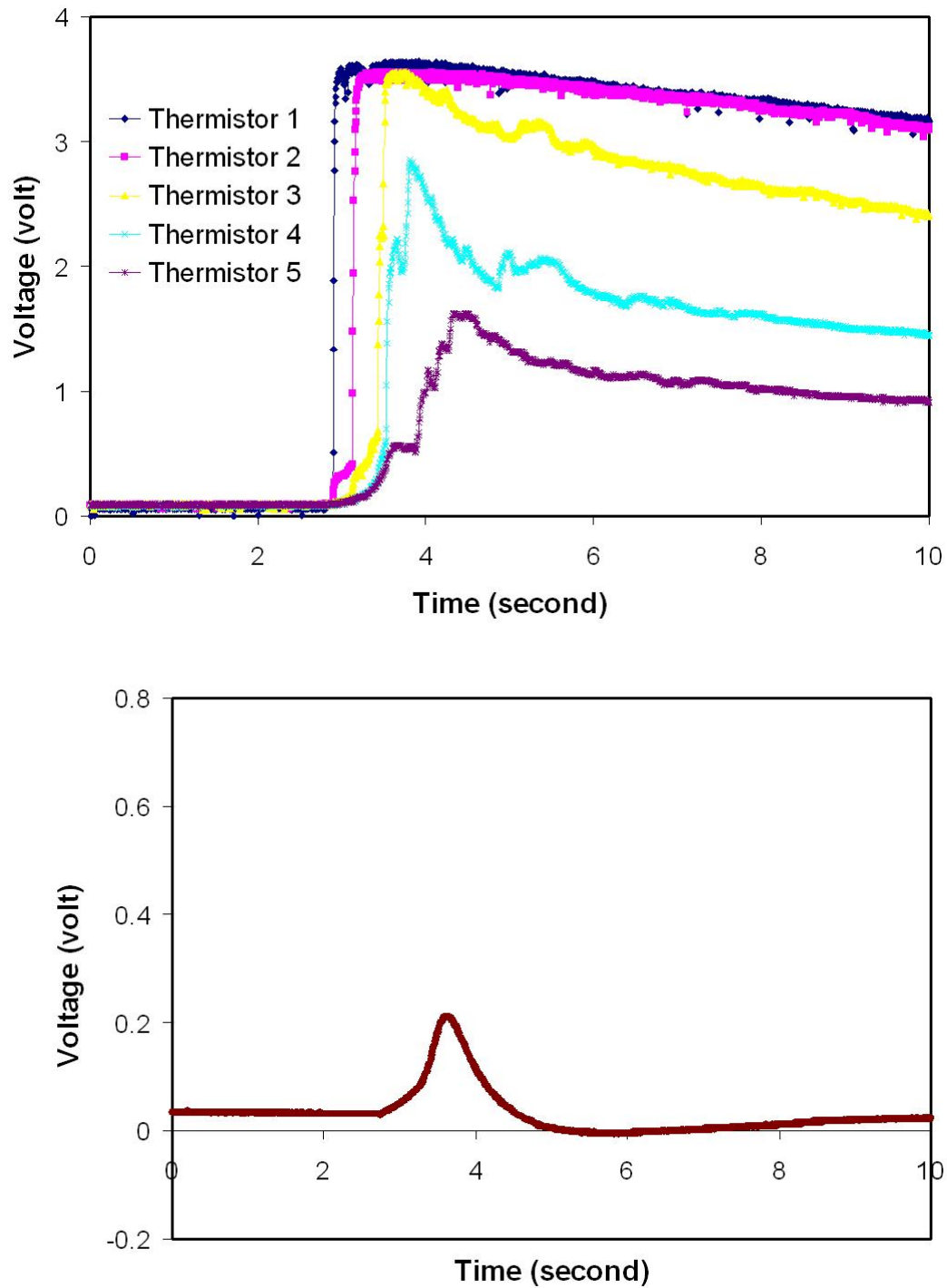


Fig. 6.6. Temperature (top) and pressure (bottom) profiles for discontinuous flame propagation combustion.

The maximum pressure rise is 6.38 psi (43.4 %), which is significantly greater than the pressure rise criterion used by ASTM methods (7 %) or the criterion used by EN 1839(B) method (5 %). The pressure rise shows that a greater proportion of the gas in the reaction vessel participated in combustion than the flash behavior examined earlier, but does not offer conclusive evidence that the flame propagated to the top of the vessel. The temperature profiles at locations along the vessel offer more detailed information. The signal profiles from the lowest thermistors (1 & 2) shows very high temperature increases (above 260 °C, the highest temperature value in thermistor data given by manufacturer) and slow cooling. Thermistor 3, which is near the center of the reaction vessel shows a sharp temperature increase, but a faster temperature drop than thermistors 1 and 2. Thermistors 4 and 5 both have similar signal profiles as thermistor 3, except their amplitudes are much lower, with maximum temperatures of approximately 95 and 60 °C respectively. The relatively low temperatures and quick cooling suggest that thermistors 3, 4, and 5 are detecting hot gases rising from below instead of flame propagating past them. The signal profiles shown for thermistors 3, 4 and 5 occur in the event of flame termination below the thermistors.

Continuous flame propagation describes a flame that propagates within the reaction vessel until it reaches the top of the vessel. Figure 6.7 shows the images from igniting 5.23 % methane in air at 14.7 psia. The images show the flame plume propagating up from the ignition source after ignition, then propagating back down, similar to discontinuous flame propagation (see fig. 6.5).





Fig. 6.7. Images from continuous flame propagation. (5.23 % methane in air)



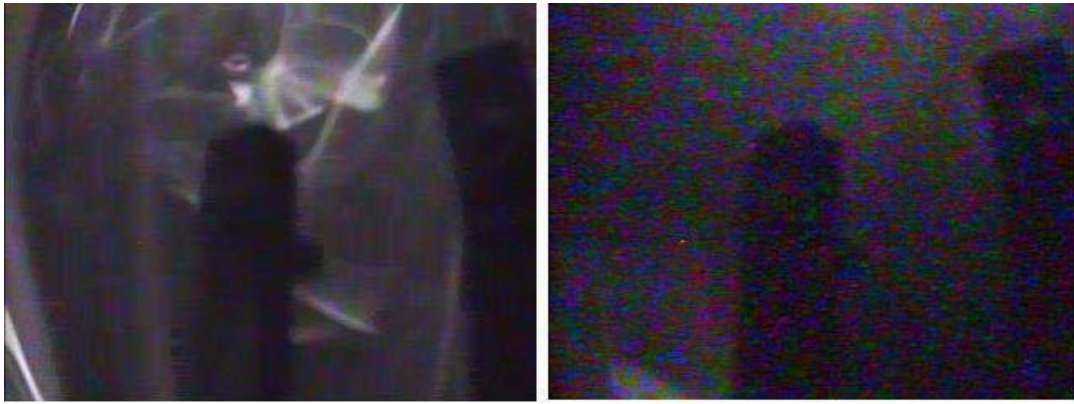


Fig. 6.7. Continued.

The video data shows that flame propagation occurred in all directions (upward, downward, and horizontal), but does not provide an objective means to distinguish discontinuous and continuous flame propagation. However, the temperature and pressure profiles show substantial differences between the two combustion behaviors.

Figure 6.8 shows temperature and pressure measurements from the combustion of 5.23 % methane in air. The pressure measurements indicate a maximum pressure rise of 16.53 psi (112 %), which is more than an order of magnitude larger than the pressure rise criterion specified by the ASTM methods (7 %) or the criterion specified by EN 1839(B) (5 %), and more than double the pressure rise from discontinuous flame propagation. All of the temperature signals increase to near the maximum signal range, similar to behavior of thermistors 1 and 2 in discontinuous flame propagation. In continuous flame propagation, the temperature rise for each thermistor in succession, and then slowly decreases as the gas around the thermistors cools.

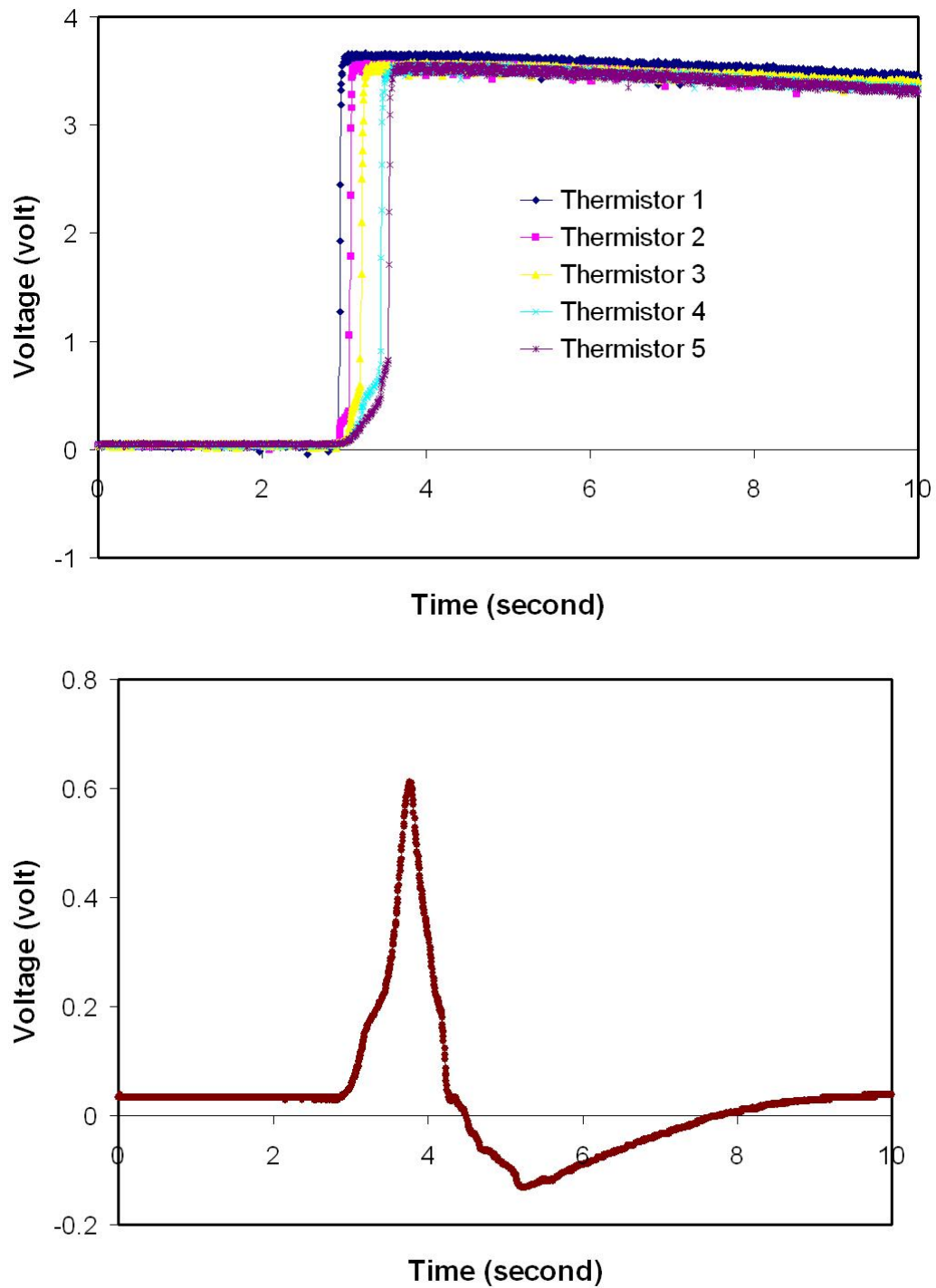


Fig. 6.8. Temperature (top) and pressure (bottom) profiles for continuous flame propagation combustion.

While the greater pressure rise is a strong indication that more gas was combusted in the experiment, the magnitude fluctuates depending upon the amount of gas combusted. If the flame terminates near the top of the reaction vessel, the pressure rise can be fairly high, creating a situation where a simple pressure criterion cannot distinguish between continuous and discontinuous flame propagation. The temperature profiles from the thermistors are the measurements that show propagation to the top of the vessel. The nearly identical signal profiles, with time delay between thermistors, show that the same thermal events that occurred at the bottom of the vessel also occurred along the entire length of the vessel. This thermistor signal profile occurs in the event of an expanded flame propagating past the thermistor. The difference between discontinuous and continuous flame propagation therefore can be inferred from the temperature profiles.

Thermistor behavior during combustion of ethylene is in good agreement with that observed during combustion of methane, with the exception of a minor discrepancy during continuous and discontinuous flame propagations. The data for combustion of 2.72 % ethylene in air is shown to illustrate this phenomenon. Figure 6.9 shows the thermistor temperature profiles for ethylene combustion with continuous flame propagation.

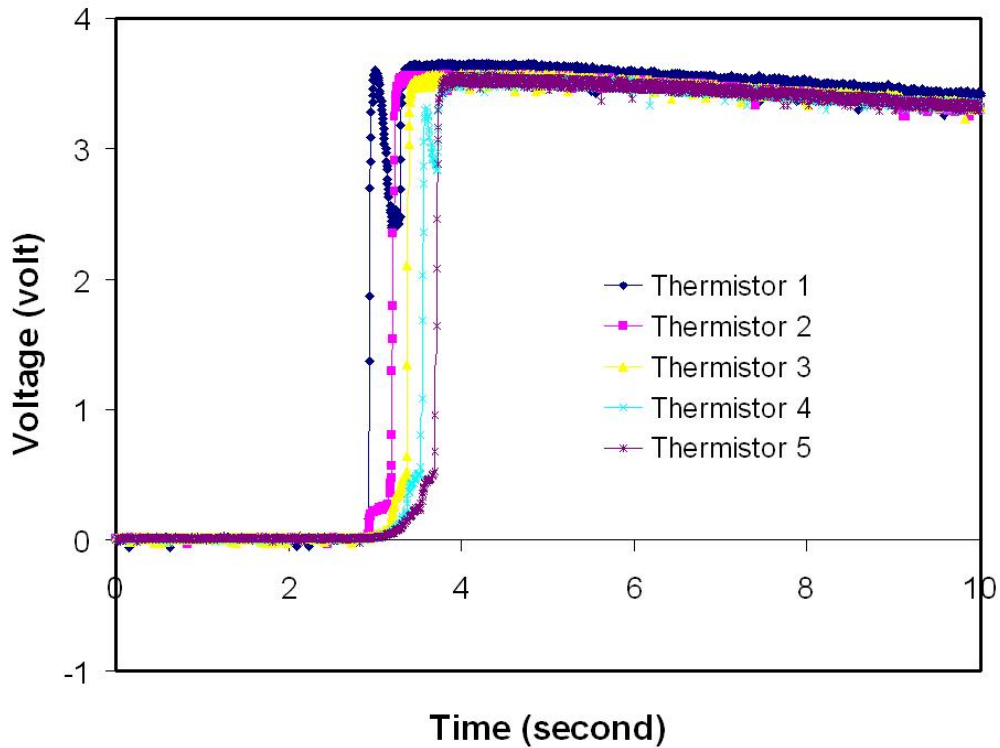


Fig. 6.9 Temperature profiles for continuous flame propagation of ethylene. (2.72 % ethylene in air)

The signal profiles of thermistors 1 and 4 both show a sharp dip before they rise to the maximum value. The other profiles match those observed with continuous flame propagation of methane (see figure 6.6), which shows that this is a continuous flame propagation as well. The signal profiles of thermistors 1 and 2 from figure 6.9 are compared in figure 6.10, which shows that they are nearly identical except for the dip.

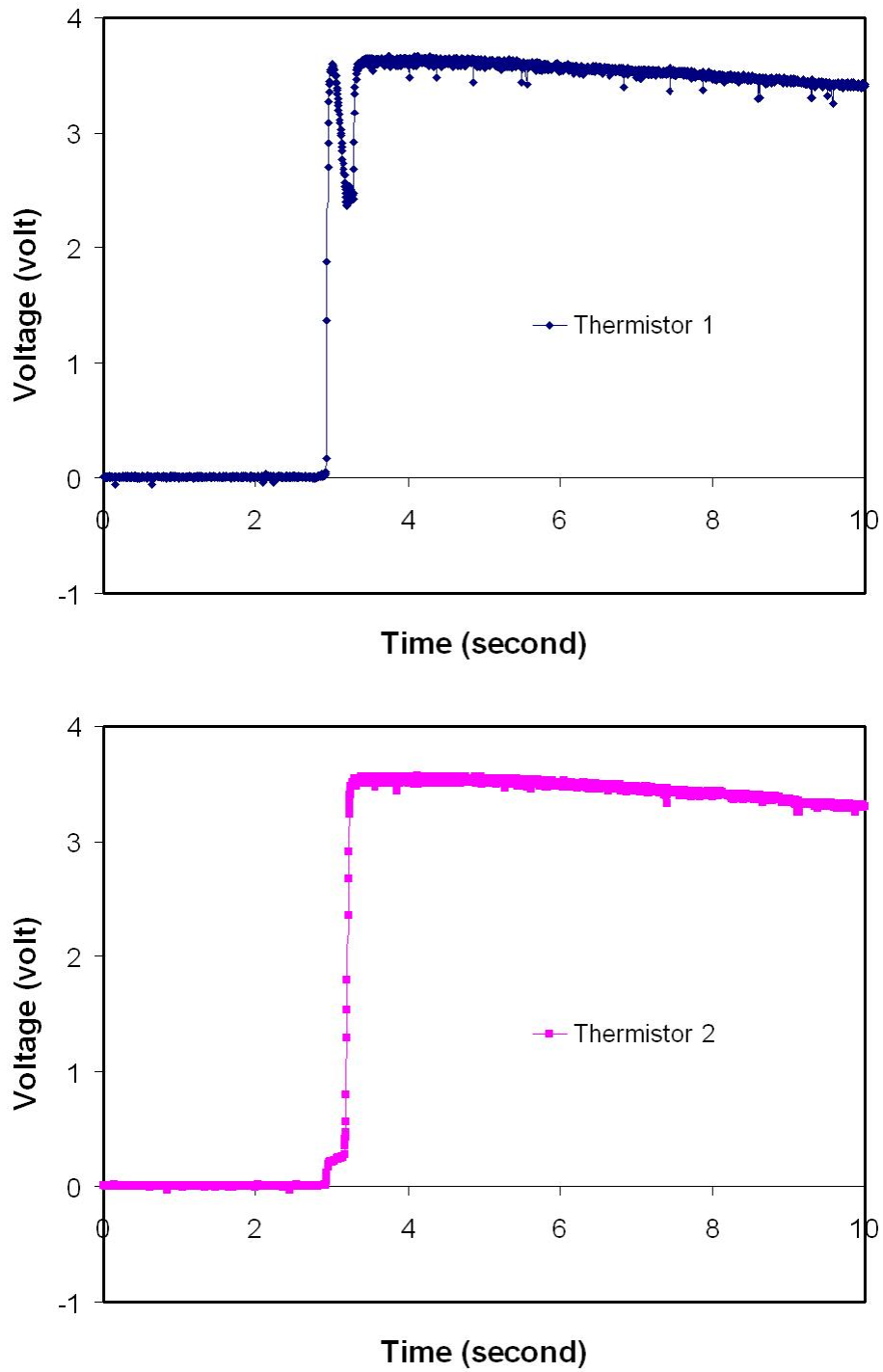


Fig. 6.10. Comparison of signal profiles for thermistors 1 and 2. (2.72 % ethylene in air)

Figure 6.11 shows the pressure data of ethylene with continuous flame propagation. The maximum pressure rise is approximately 16.1 psi (109 %). The pressure rise and the shape of the curve in figure 6.11 are not significantly different from the pressure data of methane with continuous flame propagation shown in figure 6.6.

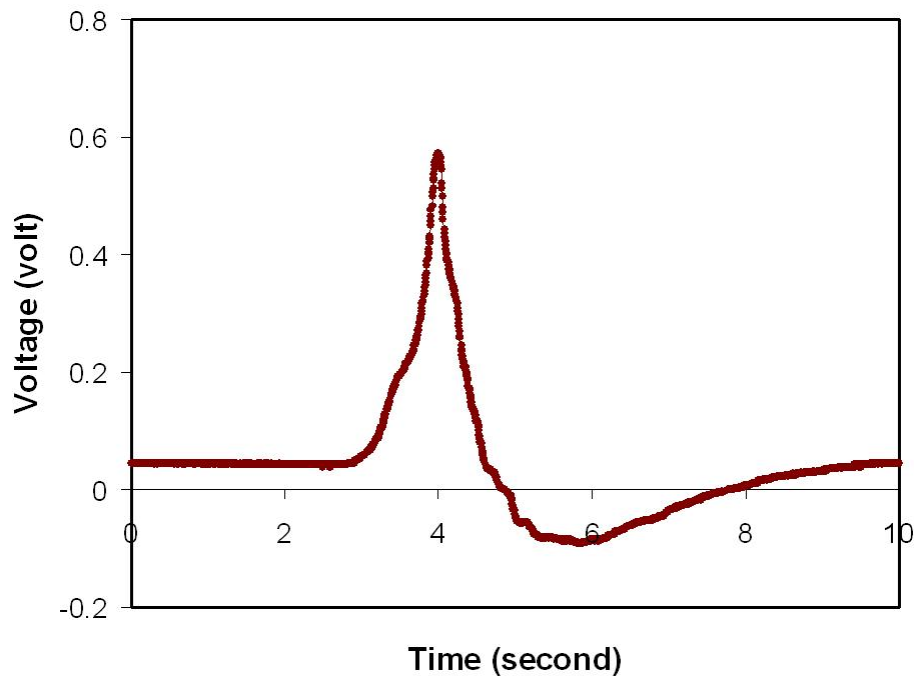


Fig. 6.11 Pressure profile for continuous flame propagation of ethylene. (2.72 % ethylene in air)

The images in figure 6.12 show the ignition, upward propagation, and then the downward propagation of the ethylene flame. The video images are similar to those of methane with continuous flame propagation, except the downward propagation occurs slightly later, approximately 0.5 s with ethylene instead of 0.3 s with methane.



Fig. 6.12. Images of continuous flame propagation of ethylene. (2.72 % ethylene in air)

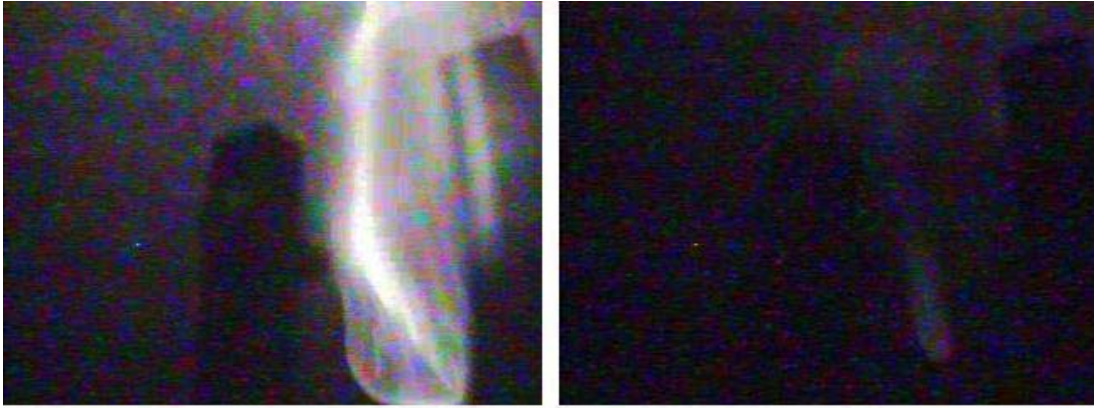


Fig. 6.12. Continued.

The video and pressure observations show only minor dissimilarities, and do not demonstrate a cause for the change in thermistor signal profiles. A possible explanation is that the ethylene flame propagates horizontally at a lower rate, leaving a greater volume of uncombusted gas around the initial flame path. The passage of the flame creates a turbulent zone where the combusted and uncombusted gas mixes, lowering the temperature temporarily until combustion resumes in the area.

It is not necessary to consider the dip in the thermistor signal profiles when determining the type of combustion behavior observed in the flammability apparatus. In addition, greater knowledge of the gas flows within the reaction vessel during combustion is necessary to resolve the question of its meaning. Therefore further analysis of this feature is outside the scope of this dissertation.



### 6.3 Thermistor signal and combustion zones

The thermistor signal profiles correspond to different zones in the reaction vessel for different combustion types. Figure 6.13 illustrates the zones and their relationship to combustion types identified in section 6.3: non-combustion, expanded flame, termination (1), and termination (2).

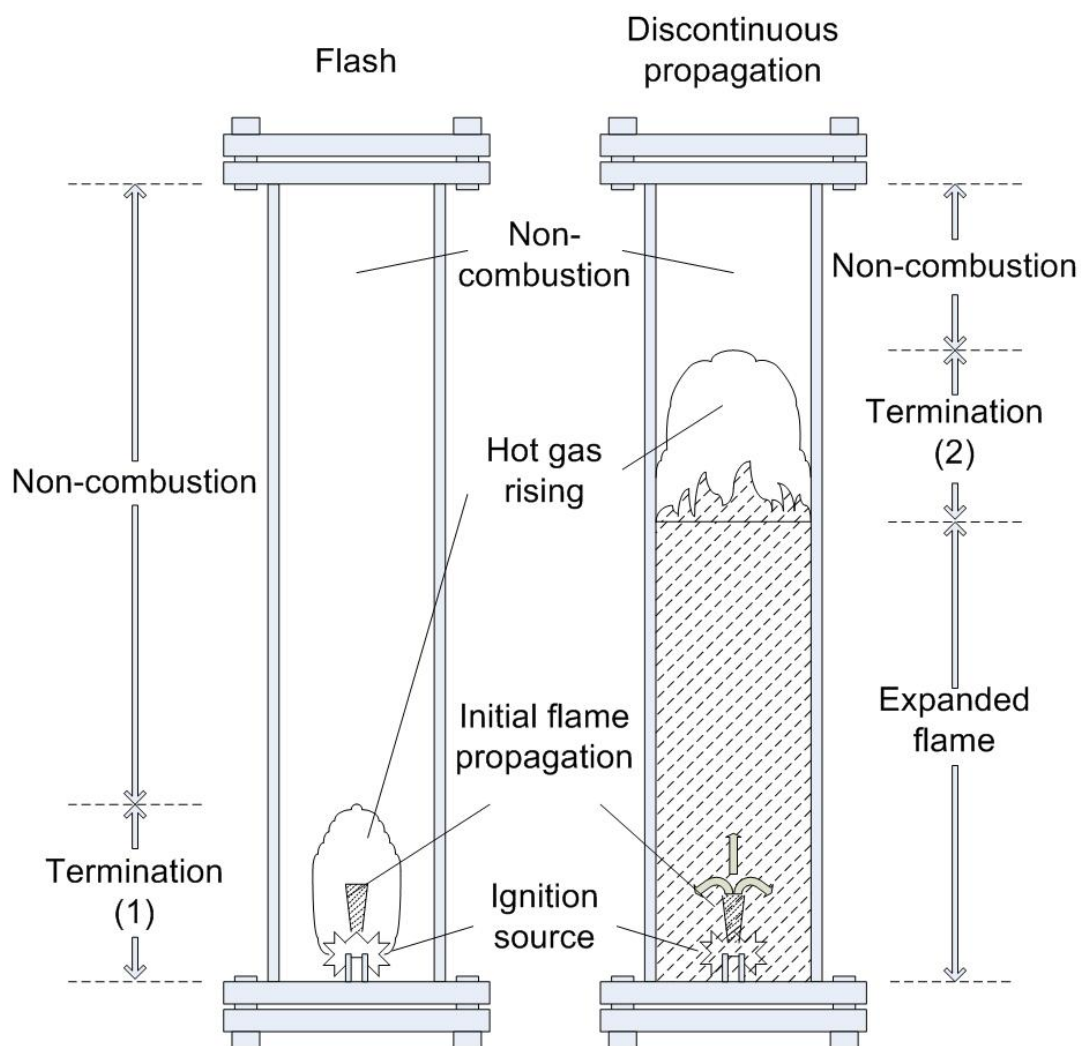


Fig. 6.13 Zones within the reaction vessel during combustion.

The non-combustion zone is the volume within the reaction vessel where the flame propagation has not reached, and with little to no hot products of combustion. The temperature in the non-combustion zone is ambient or nearly ambient. The expanded flame zone is the volume that experiences complete or near complete combustion of the gas mixture from horizontal and vertical flame propagation. The temperature in the expanded flame zone is very high, and it decreases slowly. Figure 6.14 shows generalized thermistor signal vs. time curves for non-combustion and expanded flame zones.

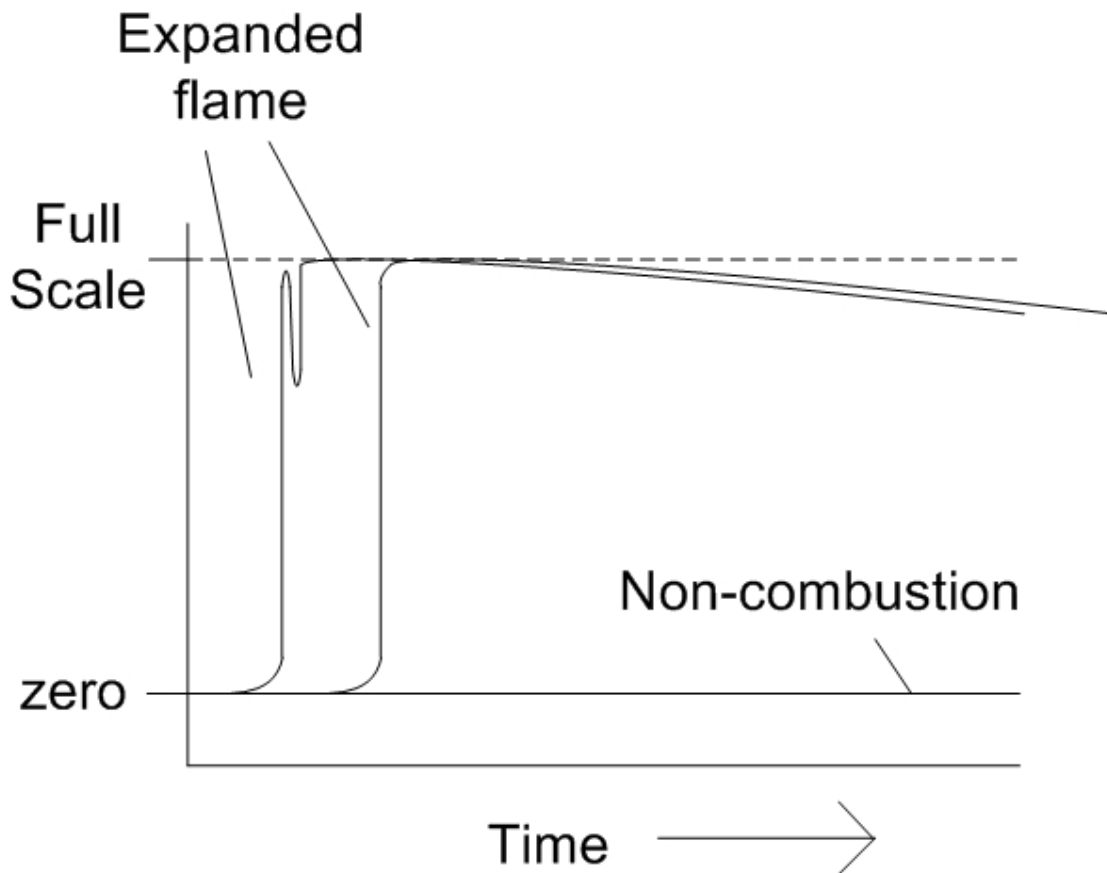


Fig. 6.14 Sample thermistor signal profiles: expanded flame and non-combustion.

The termination (2) zone is the region above the expanded flame zone, where a relatively large volume of hot gases rises into, and mixes with, unburned gases. The temperature in the termination zone (2) can be high, but it drops significantly faster than in the expanded flame zone. This produces a distinctively different thermistor signal profile than in the expanded flame zone. Figure 6.15 shows generalized thermistor signal profiles for the termination (2) zone.

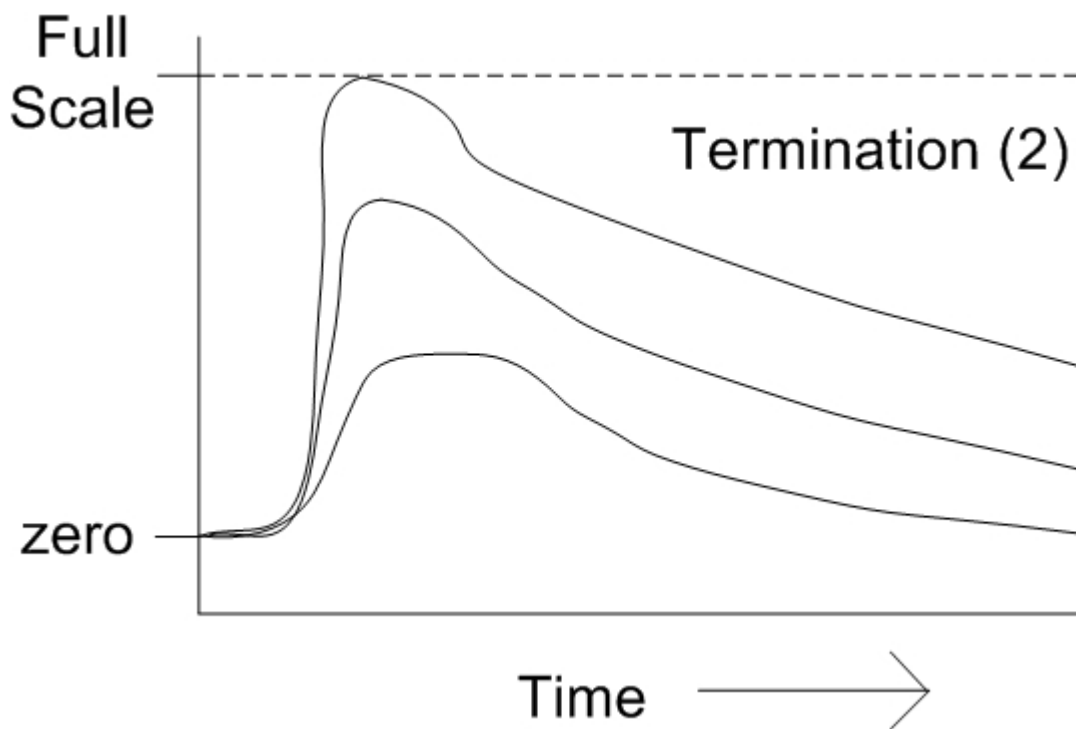


Fig. 6.15 Sample thermistor signal profiles: termination (2).

The termination (1) zone is the volume where flash combustion occurs and terminates. The heat produced by the terminated flame quickly dissipates into the

unburned gases nearby, resulting in a peak in the thermistor signal. Figure 6.16 shows generalized thermistor signal profiles for the termination (1) zone.

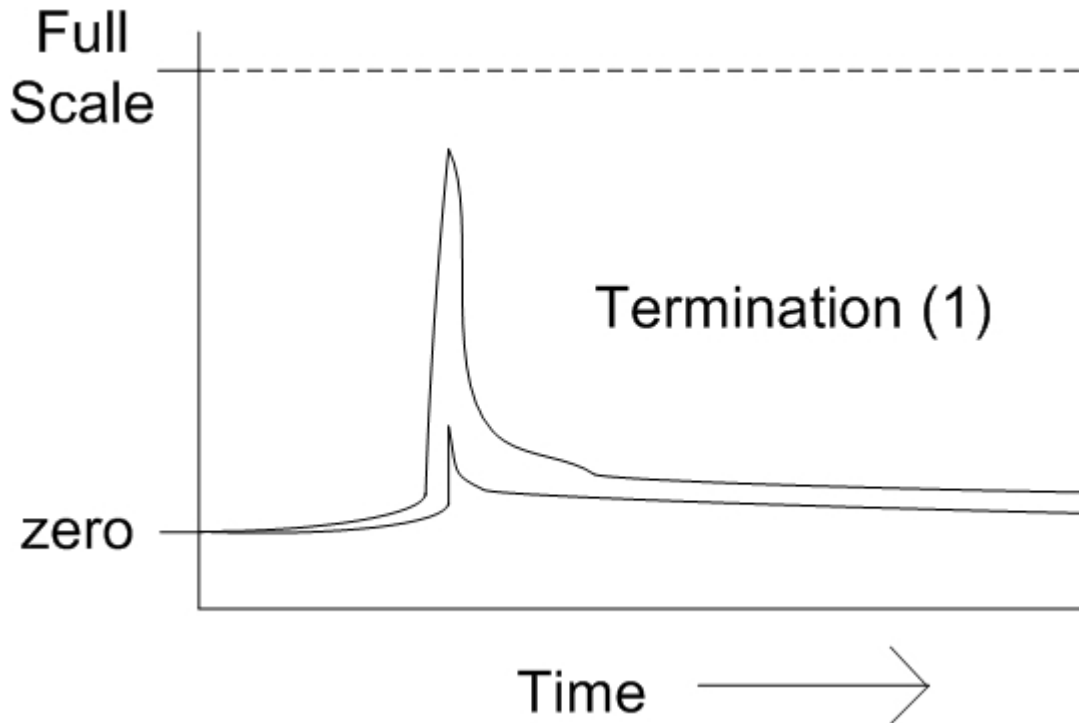


Fig. 6.16 Sample thermistor signal profiles: termination (1).

The magnitude of the temperature peak can be large or small, depending upon the distance propagated by the flame. Sometimes the signals from both thermistors 1 and 2 exhibit peaks, which indicates that the flame propagated up to or near thermistor 2 (see figure 6.17).

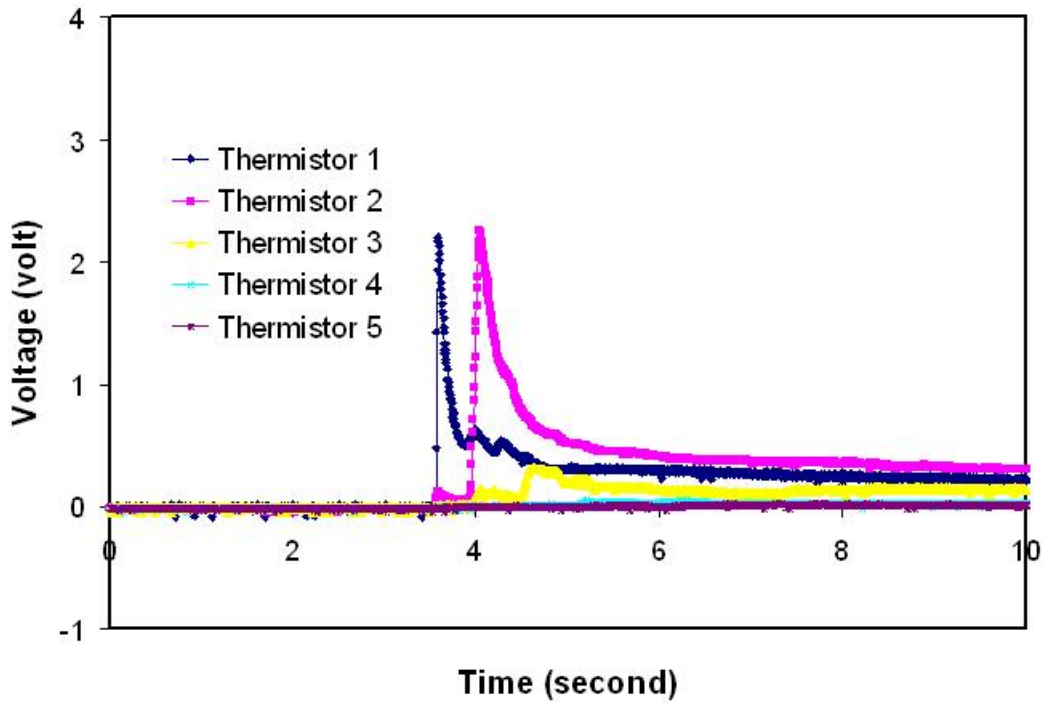


Fig. 6.17. Double temperature peaks during combustion. (4.5 % methane in air)

This phenomenon indicates when the flame propagates past thermistor 1, and in theory if a temperature peak occurs at thermistor 3 it would indicate that the flame plume propagated past thermistor 2. However, there is no signal behavior that conclusively indicates the level the flame plume propagated to, only past. An estimation of the propagation distance is thus possible, but the large uncertainty renders it unsuitable for use in measurement criteria.

#### 6.4 Thermal criterion for flammability

Determination of flammability limits requires three components: a definition of flammability, a measurement criterion to detect combustion of mixtures at various concentrations, and a method to select the flammability limit from the measurements.

American standards and authors define flammability limits as the limiting fuel concentrations where the flame can propagate through the mixture, while the European definition is the limiting concentration where the flame just fails to propagate [23]. Regardless of which definition is used, the central focus of the measurement criterion is the detection of flame propagation. The questions of how far the flame has to propagate, or what pressure changes must result from the flame propagation to indicate a flammable mixture are functions of measurement criteria, which vary from one apparatus to another.

The thermistor sensors have been demonstrated to be capable of detecting flame propagation in section 6.2, and their signal profiles matched with the combustion zones in section 6.3 for use in analysis. The reaction vessel of the flammability apparatus is a closed cylindrical vessel with ignition at the bottom, similar to open glass cylinder experiments conducted by U.S. Bureau of Mines. A measurement criterion that defines a gas mixture as flammable when the flame propagates to the top of the vessel would allow the measured limits to be compared to existing data collected in similarly shaped vessels, and to represent concentrations of fuels that can sustain combustion indefinitely.

The selection method consists of guidelines on the step size, number of experiments to be conducted and the number of propagations determined by the measurement criterion that selects the flammability limit. The selection method is an important factor in the accuracy and precision of the limits determined, as discussed in section 5.4. Flame propagation for mixtures near the flammability limit display probabilistic behaviors due to random errors in composition, fluctuations in mixture conditions (turbulence, pressure, temperature), and variation in ignition energy or power. Multiple experiments with mixtures made at the same composition can yield different results. Experiments at two compositions (within one step size of each other) that demonstrate continuous flame propagation over 50 % of the time at one composition and less than 50 % of the time at the other would indicate that the flammability limit lies somewhere in between those compositions. In the case where one composition has 0 % propagation occurrences, the composition with over 50 % propagation occurrences is selected as the flammability limit. In all other cases, the composition with less than 50 % propagation occurrences is selected for the flammability limit. Combining the selection method with a small step size (0.01 mol % for pure fuels in air, 0.02 mol % for all other mixtures), precise and conservative flammability limits can be measured.

The thermal criterion for the flammability apparatus is the detection of an expanded flame zone at the fifth thermistor (top), indicating continuous flame propagation from the ignition source at the bottom to the top of the reaction vessel. The lower flammability limit is the highest concentration where four or less flame

propagations are detected with the thermal criterion, and *vice versa* for the upper flammability limit.

### 6.5 Flammability of hydrocarbons in air

The flammability of several hydrocarbon gases were determined in air at atmospheric pressure (14.7 psia), 22.5 °C using the thermal criterion. The experimental results are summarized in table 6.1.

Table 6.1.  
Combustion of hydrocarbons in air at and near the flammability limit

	Fuel conc. (mol %)	Continuous Flame Propagation		
		(%)	Number of propagations	Number of experiments
methane	5.23*	40	4	10
	5.24	100	5	5
	15.77	62.5	5	8
	15.78*	25	2	8
ethane	2.72*	14.3	1	7
	2.73	55.6	5	9
propane	2.09*	14.3	1	7
	2.10	83.3	5	6
butane	1.72*	40	4	10
	1.73	83.3	5	6
ethylene	2.70	0	0	2
	2.71*	14.3	1	7
	2.72	55.6	5	9
	30.19	100	5	5
	30.20*	33.3	3	9
propylene	2.26	0	0	6
	2.27*	55.6	5	9

\* Selected flammability limit concentration.



The experimentally determined LFLs and some values reported in the literature are summarized in table 6.2. All reported limits are given as mole fractions in per cent.

Table 6.2.  
Lower flammability limits (fuel concentrations) of hydrocarbons in air

	This Work (mol %)	Previous Workers (mol %)	Apparatus type
Methane	5.23	5.3	Vertical glass cylinder[12]
		4.85	20 L sphere, 7 % pressure rise[29]
		4.3	EN 1839 (T) [25]
		4.9	EN 1839 (B) [25]
		4.66	Counterflow burner[20]
Ethane	2.72	3.0	Vertical glass cylinder[12]
		2.53	20 L sphere, 7 % pressure rise[8]
		2.9	Counterflow burner[20]
Propane	2.09	2.2	Vertical glass cylinder[12]
		1.93	20 L sphere, 7 % pressure rise[8]
		2.249	Counterflow burner[20]
Butane	1.72	1.9	Vertical glass cylinder[12]
		1.55	20 L sphere, 7 % pressure rise[8]
Ethylene	2.71	3.05	Vertical glass cylinder[12]
		2.62	20 L sphere, 7 % pressure rise[29]
		2.4	EN 1839 (T) [25]
		2.6	EN 1839 (B) [25]
Propylene	2.27	2.4	Vertical glass cylinder[12]

The upper flammability limits of methane and ethylene also were determined.

Table 6.3 summarizes the results and compares them with values reported in the literature.

Table 6.3.  
Upper flammability limits (fuel concentrations) of methane and ethylene

	This work (mol %)	Previous Workers (mol %)	Apparatus type
Methane	15.78	14	Vertical glass cylinder[12]
		16.14	20 L sphere, 7 % pressure rise[29]
		16.8	EN 1839 (T) [25]
		16.9	EN 1839 (B) [25]
Ethylene	30.20	28.6	Vertical glass cylinder[12]
		30.38	20 L sphere, 7 % pressure rise[29]
		32.6	EN 1839 (T) [25]
		27.4	EN 1839 (B) [25]

The experimental results from the new apparatus generally fall between the values measured by the U.S. Bureau of Mines using vertical glass cylinders with visual criterion of flame propagation to the top, and results measured with 20 L spheres with 7 % pressure rise criterion or 14 L spheres with 5 % pressure rise criterion (EN 1839(B)). This demonstrates that the new apparatus provides a reasonable level of accuracy.

The results from the EN 1839 (T) apparatus (glass cylinder with 10 cm vertical propagation criterion) show much wider flammability ranges for methane and ethylene. This is not unexpected because of the difference in the measurement criteria. Flash combustions within the new apparatus often produced temperature peaks that indicated flame propagation reached the level of thermistor 2 (26 cm from ignition source) or at least past thermistor 1 (10 cm from ignition source). The gas mixtures exhibiting those combustions are not considered flammable by the criteria used in this study, but they would satisfy the EN 1829 (T) criterion. For example, 4.26 mol % methane and 2.58

mol % ethylene are fuel concentrations just below the concentrations where double temperature peaks occur after ignition. However, because the thermistor signals do not represent a way to precisely measure flame propagation distance for small flames, such determinations would be highly subjective.

The differences with the results from the counterflow burner apparatus are more difficult to explain. The flammability limits determined by counterflow burner apparatuses are obtained by extrapolating the fuel concentration to zero stretch rate, instead of direct determination of flame propagation or the lack thereof. The counterflow burner does not share apparatus parameters such as vessel shape, size, or ignition energy with other apparatuses. Instead its parameters are nozzle size and nozzle distance because it measures stretch rates from already burning twin jet flows of gas from the nozzles aimed at each other. There is no explanation as to why the methane lower flammability limit measured is higher than the counterflow results, while the ethane and propane lower flammability limits are lower (see table 6.1).

## 6.6 Comparison of fuel mixture flammability limits with counterflow data

Under certain conditions, flammability limits determined using the counterflow method are not consistent with other experimental data. A recent study by Subramanya *et al.* [20] using a counterflow apparatus suggests that the lower flammability of methane-ethane and methane-propane fuel mixtures have large deviations from values

predicted using Le Chatelier's rule. Their result contradicts values obtained by Coward *et al.* in open glass cylinders [21] (see figure 3.1). The results are unusual since Le Chatelier's rule is known to give reasonably good estimates of the lower flammability for many fuel mixtures, though there are notable deviations when applied to upper flammability limits [15].

The lower flammability limits of methane-propane and methane-butane mixtures also were determined with the new apparatus. The methane-propane data enables comparison with the counterflow data, and the methane-butane data enables comparison with open glass cylinder data and the counterflow data. Methane-ethane mixtures were not investigated because such mixtures have been characterized in natural gas related studies [12]. There are few recent works that deal with the lower flammability of butane mixtures.

Table 6.4 shows the experimental results from the combustion of methane-propane and methane-butane mixtures determined using the new apparatus.

Table 6.4  
Combustion of methane/propane and methane/butane mixtures in air

	Fuel conc. (mol %)	Continuous Flame Propagation		
		(%)	Number of propagations	Number of experiments
50/50 methane/propane	3.04*	25	2	8
	3.06	83.3	5	6
75/25 methane/propane	3.88*	14.3	1	7
	3.90	62.5	5	8
24/76 methane/butane	2.09*	33.3	3	9
	2.11	83.3	5	6
49/51 methane/butane	2.56*	14.3	1	7
	2.58	71.4	5	7
75/25 methane/butane	3.50*	14.3	1	7
	3.52	100	5	5

\*Selected flammability limit concentration.

Figure 6.18 shows the experimental and calculated lower flammability limits of methane-propane and methane-butane mixtures determined by the new apparatus, counterflow apparatus [20], and Coward *et al.* [21]. The curves in figure 6.18 are calculated from pure component flammability limits using Le Chatelier's rule:

$$L_m = \frac{100}{\sum_{i=1}^n \frac{Y_i}{L_i}} \quad (6.1)$$

$L_m$  is the flammability limit of the fuel mixture in air in volume %.  $L_i$  is the corresponding flammability limit for the fuel component  $i$  in volume %.  $Y_i$  is the corresponding volume fraction of the fuel component  $i$  in the fuel mixture in volume %.

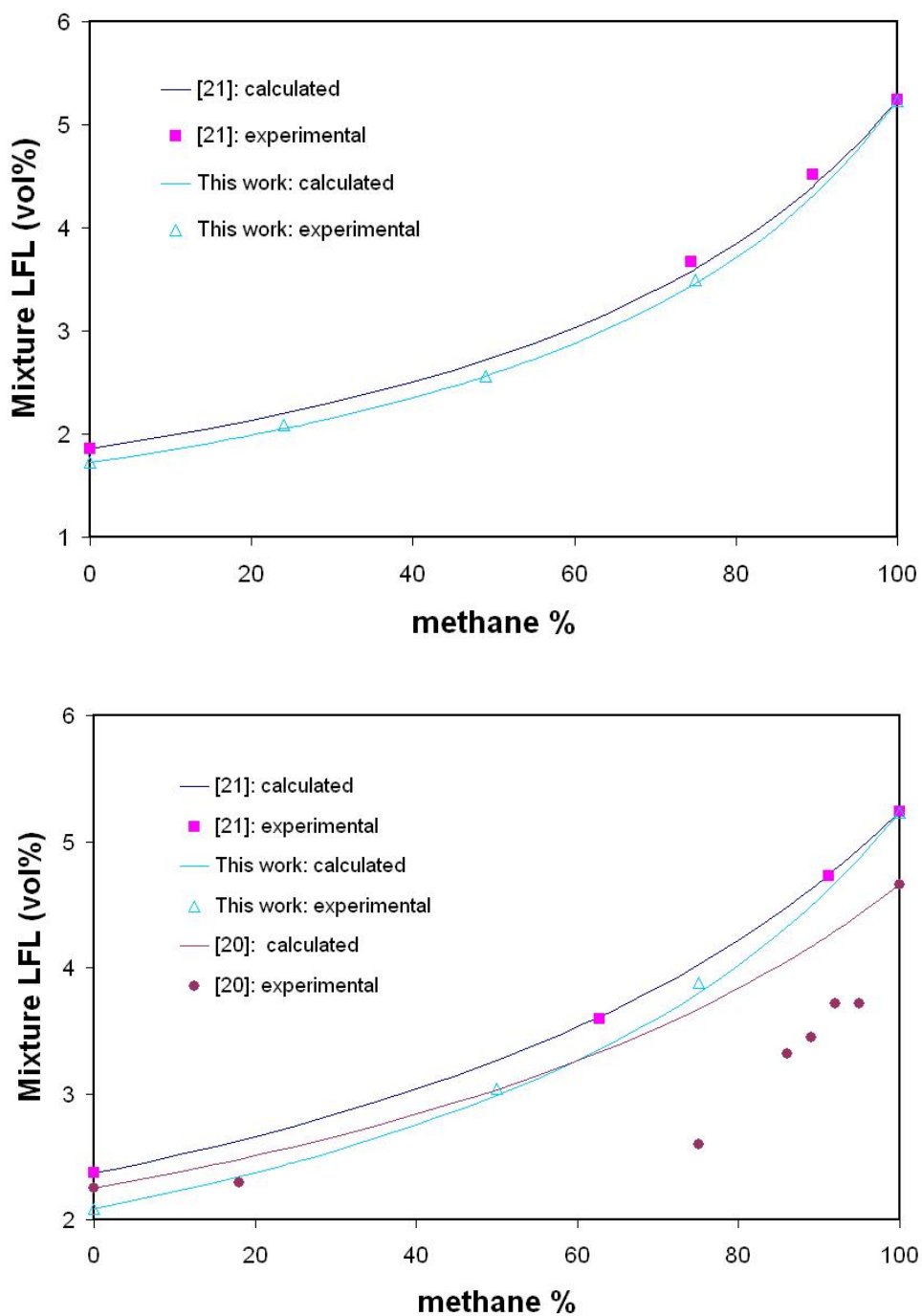


Fig. 6.18. Comparison of Le Chatelier predictions with experimental LFLs for methane/butane (top) and methane/propane (bottom) mixtures in air.

Le Chatelier's rule predictions agree well with the flammability limits determined in this work, as is the case for the results of Coward *et al.* [21]. Figure 6.19 compares Le Chatelier's rule predictions with measured flammability limits. The largest deviations for Le Chatelier's rule predictions are less than 0.1 % for the flammability limits determined by Coward *et al.* [21] and in this work. On the other hand, the limits determined with the counterflow apparatus have maximum deviations from Le Chatelier's rule of 1.1 % for methane-ethane mixtures and for methane-propane mixtures.

It is clear that the mixture flammability measurements made using the counterflow apparatus are inconsistent with measurements made using the more common cylindrical type apparatuses with respect to the applicability of Le Chatelier's rule. The consistency between the results of Coward, *et al.* [21], and the results reported here strongly support the use of Le Chatelier's rule for practical applications. Currently it is unknown if it is the dissimilar apparatus parameters or the method of extrapolation (or both) that is responsible for the discrepancies in the counterflow results of Subramanya *et al.* [20].

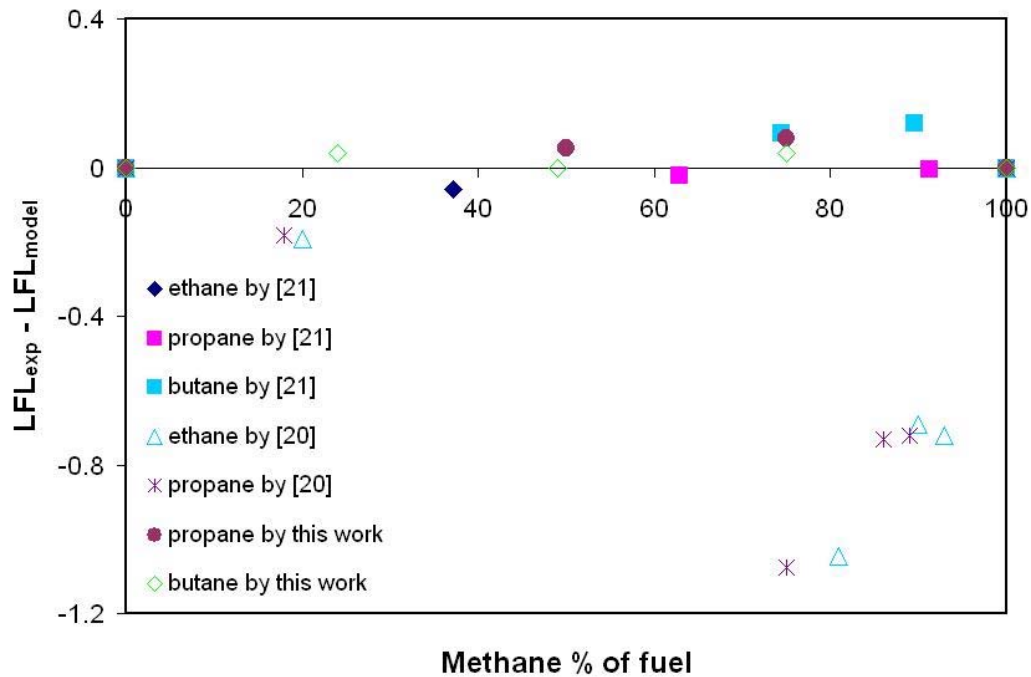


Fig. 6.19. Mixture LFL deviations from Le Chatelier's rule predictions.

### 6.7 Flammability in atmospheres with reduced oxygen concentration

A standard tactic in dealing with the hazards of flammable gas releases is the addition of one or more inert gases in order to lower the fuel concentration below the lower flammability limit of that fuel in the specific atmosphere, usually air. The addition of inert gases lowers both the fuel concentration and the oxygen concentration at the same time. The LFL of the fuel increases and the UFL decreases when the oxygen concentration is reduced, eventually converge at the minimum oxygen concentration (MOC) necessary for combustion of the fuel of interest.



Table 6.5.  
Combustion of methane, butane, and methane/butane mixture in atmosphere with reduced oxygen concentration

	O <sub>2</sub> conc. (mol %)	Fuel conc. (mol %)	Continuous Flame Propagation		
			Propagation Occurrence Rate (%)	Number of Propagations	Number of Experiments
CH <sub>4</sub>	11.9**	5.70	0	0	6
	11.9**	5.72*	55.6	5	9
	11.9**	5.74	0	0	6
	12.1	5.40	0	1	0
	12.1	5.50	100	1	1
	12.1	5.60	100	1	1
C <sub>4</sub> H <sub>10</sub>	10.6**	2.04	0	0	6
	10.6**	2.06*	62.5	5	8
	10.6**	2.08	0	0	6
	10.7	2.04	100	1	1
	10.7	2.06	100	1	1
	10.7	2.08	100	1	1
50/50 CH <sub>4</sub> /C <sub>4</sub> H <sub>10</sub>	21.0	2.58*	14.3	1	7
	21.0	2.60	83.3	5	6
	17.0	2.58*	25	2	8
	17.0	2.6	71.4	5	7
	13.5	2.64*	14.3	1	7
	13.5	2.66	100	5	5
	12.5	2.74*	33.3	3	9
	12.5	2.76	83.3	5	6
	11.5	2.82*	14.3	1	7
	11.5	2.84	55.6	5	9
	11.0	2.86*	14.3	1	7
	11.0	2.88	83.3	5	6
	10.7**	2.94	0	0	6
	10.7**	2.96*	55.6	5	9
	10.7**	2.98	0	0	6
	10.6	2.94	0	0	1
	10.6	2.96	0	0	1
10.6	2.98	0	0	1	

\* denotes LFL concentrations, and \*\* the minimum oxygen concentrations.

The lower flammability limit of an equimolar methane-butane mixture was measured as a function of oxygen concentration in oxygen/nitrogen atmospheres. The MOC also was determined for the methane/butane mixture, methane, and butane (selected as the oxygen concentration where the LFL and the UFL converges). Table 6.5 summarizes the experimental results.

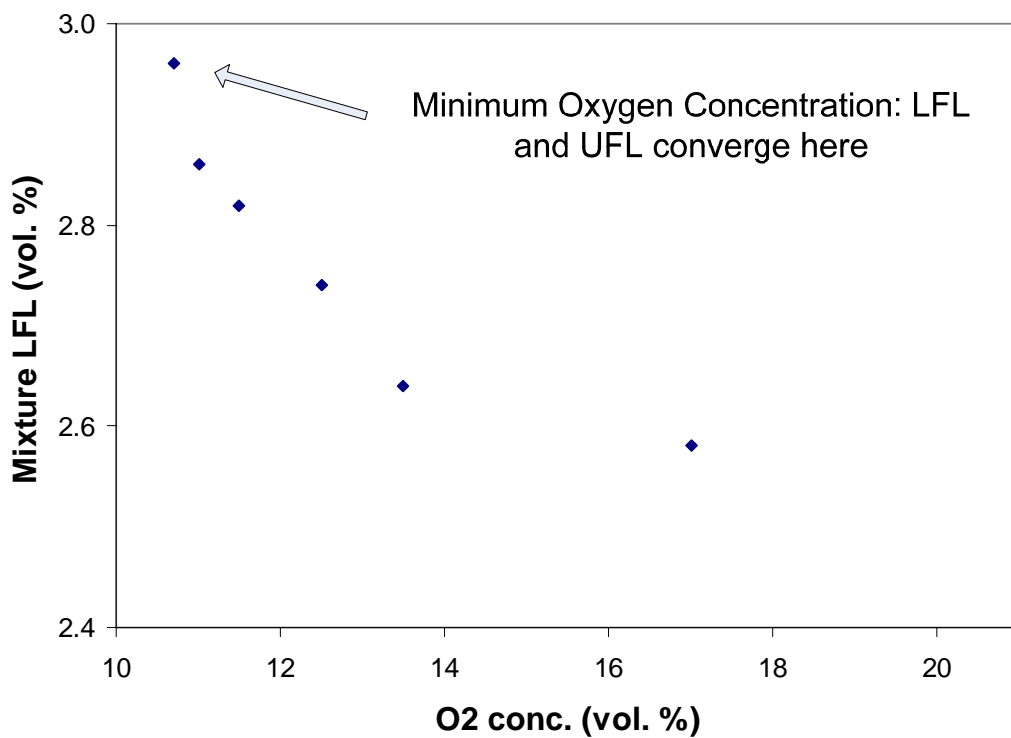


Fig. 6.20. Experimental LFL of 50/50 methane-butane mixture within a reduced oxygen atmosphere.

Figure 6.20 shows that the mixture lower flammability limit does not change appreciably until the oxygen concentration decreases to approximately 14%, then it gradually increase until the MOC (10.7 vol %) is reached.

The MOC of the methane-butane mixture in this work is lower than the values produced by previous work in glass cylindrical vessels. The MOC measured for pure butane in this work is somewhat lower than a previously reported value and slightly lower than the mixture MOC (see table 6.6).

Table 6.6.  
Comparison of minimum oxygen concentration values

	MOC (mol%) from this work	MOC (mol%) from vertical glass cylinder vessel [12]
methane	11.9	12.8
butane	10.6	12.1
50/50 methane-butane	10.7	N/A

MOC measurements using 20 L spheres and 7% pressure rise criterion also have lower MOC values, with the mixture MOC similar in value with the pure component that has the lower MOC (see table 6.7).

Table 6.7.

Comparison of minimum oxygen concentration values found in previous works

	MOC (mol%) from 20 L spherical vessel [29]	MOC (mol%) from vertical glass cylinder vessel [12]
methane	11.6	12.8
ethylene	9.3	10
50/50 methane-ethylene	9.4	N/A

The MOC values are reasonable in view of the general trend among the literature data. The flammability limits from previous work using vertical glass cylinders are not as wide as the limits determined using spherical vessels and pressure rise criteria. The flammability apparatus developed in this work combines features from the older works (vessel shape and propagation to the vessel top) and more recent methods (fuse wire explosion for high power ignition, greater vessel width). It is reasonable for the MOC values to fall between values produced by the vertical glass cylinder vessels and the spherical vessels, following the pattern observed with other flammability values determined with the new apparatus and criteria.

## 6.8 Summary

We have demonstrated that the new apparatus can detect expanded flame propagation, and distinguish it from other phenomenon occurring within the reaction vessel by utilizing the thermistor sensors. It can detect and distinguish between discontinuous and continuous flame propagation, which enables the application of the

thermal criterion developed for flammability measurement. The flammability limits measured in air for selected pure fuel gases and fuel gas mixtures agree well with work reported previously. The limits of the gas mixtures are compared to limits obtained with open glass cylinder experiments and counterflow apparatus experiments by examining their deviations from Le Chatelier's rule. The minimum oxygen concentrations for methane, butane, and an equimolar methane-butane mixture also were measured. The methane and butane results agree with previously reported results. There are no reports of measured MOC for the equimolar mixture. The lower flammability limits of the equimolar methane-butane mixture were measured as a function of decreasing oxygen concentration.

## 7. SUMMARY AND RECOMMENDATIONS

### 7.1 Summary

The purpose of this research is to develop an apparatus capable of measuring flammability limits for a range of conditions including mixtures, varying oxygen concentration, and extended pressure and temperature ranges. Three objectives are achieved for this purpose: design and construction of a flammability apparatus with a closed cylindrical reaction vessel; examination of the combustion behavior within the vessel with visual, pressure, and thermal sensors to develop a thermal criterion for flammability limit determination; and comparison of flammability limits determined using the thermal criterion with limits determined using pressure and visual criteria that have been reported in the literature.

The resulting flammability apparatus is able to detect combustion within the reaction vessel by visual, pressure, and thermal sensors. The apparatus has a reaction vessel with shape and size comparable to vertical glass cylinder vessels used by other workers and a short cycle time for data collection.

Combustion behavior within the reaction vessel is observed using visual, pressure, and thermal sensor data, and categorized into four types: non-propagation, flash, discontinuous flame propagation, and continuous flame propagation. The visual and pressure measurements were found to be incapable of distinguishing between discontinuous and continuous flame propagation. Different zones during combustion

within the reaction vessel are identified: non-combustion, expanded flame, termination (1) and termination (2). Thermal sensor signal profiles are related to the combustion zones, allowing determination of combustion types with thermal sensors alone. The thermal criterion is developed for the determination of flammability limits with the new apparatus based upon what to measure (definition of flammability) and how to measure (thermal sensor signal profiles).

The flammability limits of the following gases were determined using the thermal criterion:

- Methane (LFL and UFL)
- Ethane (LFL)
- Propane (LFL)
- Butane (LFL)
- Ethylene (LFL and UFL)
- Propylene (LFL)

The lower flammability limits of the following gas mixtures in air were determined and predictions from Le Chatelier's rule compared with the experimental results:

- methane-propane
- methane-butane

The minimum oxygen concentrations of the following gases and mixtures were measured:

- methane
- butane

- equimolar methane-butane mixture

Lastly, the lower flammability limits of the equimolar methane-butane mixture were measured in atmospheres with reduced oxygen concentrations and the minimum oxygen concentration required to support combustion was determined.

The flammability limits of pure fuel gases fall between values determined using vertical glass cylinder apparatuses and spherical apparatuses, which indicates a reasonable level of agreement with the general body of flammability data. The lower flammability limits of the gas mixtures correlate well with predictions by Le Chatelier's rule, revalidating the simple model against dissenting results from recent studies made using counterflow-type apparatuses. The minimum oxygen concentration of methane and butane are lower than values found with vertical glass cylinder vessels, but the methane MOC value is close to MOC value from a spherical apparatus. The MOC for the equimolar methane mixture is very close the MOC for pure butane, which has the lower MOC of the two pure constituents.

The results of this work show that the flammability data determined with thermal criteria have an acceptable level of accuracy. The flammability apparatus is capable of producing wider (higher UFL, lower LFL) flammability limits values if a more lenient thermal criterion is used.



## 7.2 Recommendations

Experience acquired during the experiments suggests possible improvements to the flammability apparatus that have not been implemented to date. A new flammability apparatus design is proposed that should improve accuracy and data acquisition cycle time, as well as settling unresolved issues.

In the modified design, the reaction vessel remains a steel cylinder sealed by bolted flanges at both ends, but the vessel is not mounted by the top plate to an enclosure structure. Instead, it is clamped by the body and suspended in the air by metal supports connected to a stand with a wide base (see figure 7.1)

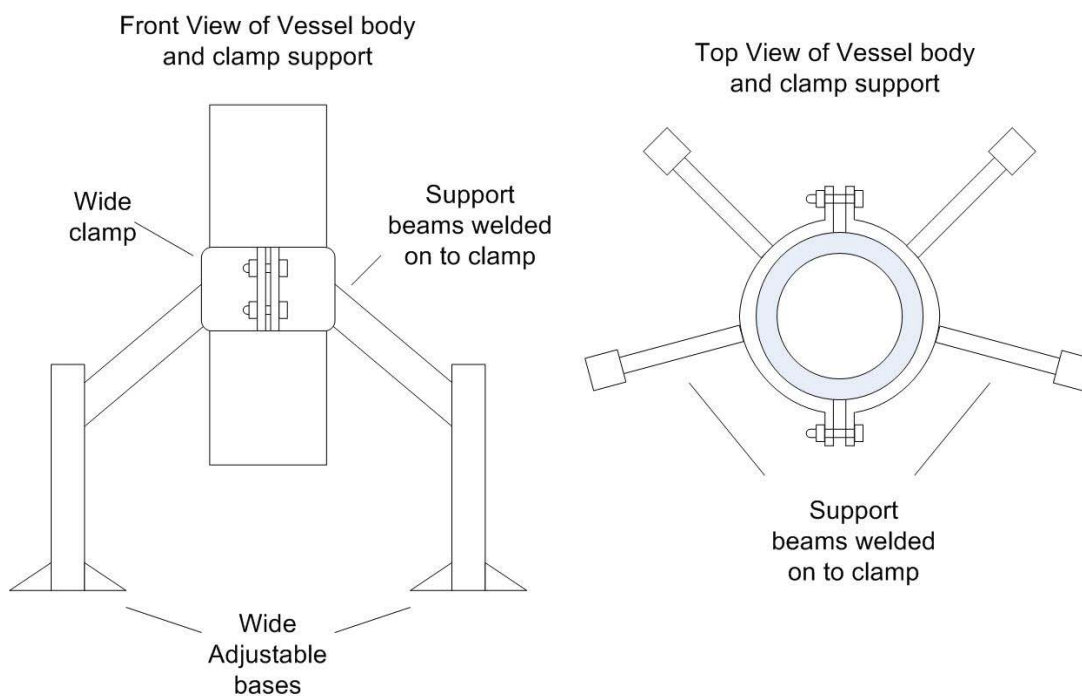


Fig. 7.1. Recommended reaction vessel body setup.

The top flange will have a recessed portion to allow for the installation of a thermistor rack consisting of a circular ring to set into the recess, a structure of metal rods to hold the thermistors at desired locations, with the wiring leading to a signal connector that can connect to a feedthrough on the bottom plate of the reaction vessel instead of the top to avoid excess wiring hanging in the path of flame propagation (see figure 7.2).

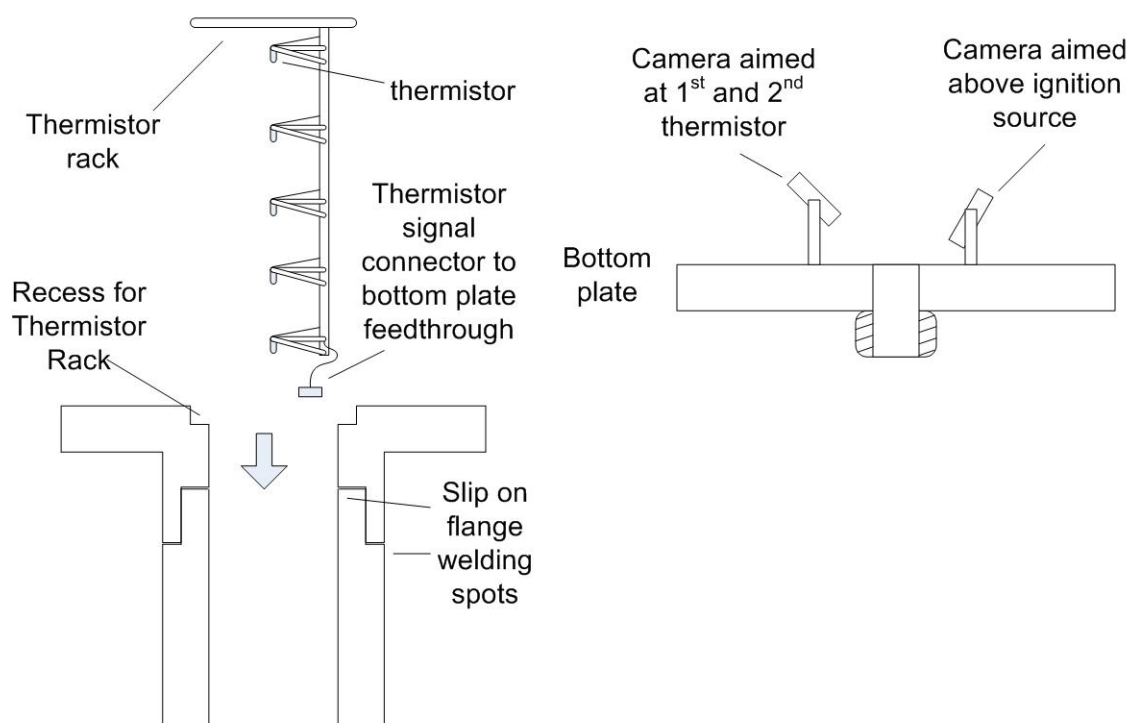


Fig. 7.2 Recommended thermistor rack and new bottom plate setup.

This new setup has a couple of advantages over the current design: it will allow for easier thermistor maintenance and modification, because the entire structure can be removed; and the vessel body no longer needs to be moved during maintenance, thus minimizing the weight-related hazards. When the safety hazard associated with weight is removed, a thicker vessel wall can be selected to reduce the risk of vessel rupture due to pressure, thus removing the need for a reaction vessel enclosure. The vessel also can have a larger diameter to accommodate experiments using gas mixtures with larger quenching distances. The addition of an extra camera to capture images above that of the first camera offers potential insights into the propagation behavior of the flame plume that forms immediately after ignition. The camera position within the vessel can be higher to provide face-on view of the interested area, yet without intruding in the flame plume's path, if the vessel body is sufficiently wide. This can provide insight as to when and where the flame plume terminates during flash combustion, as well as when and where the flame plume expands in the cases of discontinuous and continuous flame propagation.

## REFERENCES

- [1] J. L. Scheffey, D. C. Tabar, Hazard Rating System for Flammable and Combustible Liquids, *Process Safety Progress* 15(4) (1996) 230-236.
- [2] L. G. Britton, Two Hundred Years of Flammable Limits, *Process Safety Progress*, 21(1) (2002) 1-11.
- [3] ASTM E502-84, Standard Test Method for Selection and Use of ASTM Standards for the Determination of Flash Point of Chemicals by Closed Cup Methods, American Society for Testing and Materials, 1994.
- [4] ASTM D1310-86, Standard Test Method for Flash point and Fire Point of Liquids by Tag Open-Cup Apparatus, American Society for Testing and Materials, 1997.
- [5] ASTM D56-98a, Standard Test Method for Flash Point by Tag Closed Tester, American Society for Testing and Materials, 1999.
- [6] MSDS Hyperglossary, <http://www.ilpi.com/msds/ref/flashpoint.html>, (2004).
- [7] L. G. Britton, Avoiding Static Ignition Hazards in Chemical Operations, AICHE, CCPS Concept Book, New York, (1999) 84-85.
- [8] G. D. De Smedt, D. De Corte, R. Notele, J. Berghmans, Comparison of two Standard Test Methods for Determining Explosion Limits of Gases at Atmospheric Conditions, *Journal of Hazardous Materials*, A70 (1999)105-113.
- [9] M. G. Zabetakis, Flammability Characteristics of Combustible Gases and Vapors. Bulletin 627, Bureau of Mines, 1965.

- [10] D. Kong, D. J. am Ende, S. J. Brenek, N. P. Weston, Determination of Flash Point in Air and Pure Oxygen Using an Equilibrium Closed Bomb Apparatus, *Journal of Hazardous Materials*, 102(2-3) (2003) 155-165.
- [11] A. Takahashi, Y. Urano, K. Tokuhashi, S. Kondo, Effects of Vessel Size and Shape on Experimental Flammability Limits of Gases, *Journal of Hazardous Materials*, A105 (2003) 27-37
- [12] H. F. Coward, G. W. Jones, Limits of Flammability of Gases and Vapors, US Bureau of Mines Bulletin, Bulletin 503, Washington, DC, 1952
- [13] J. M. Kuchta, Investigation of Fire and Explosion Accidents in the Chemical, Mining, and Fuel-Related Industries – a Manual, Bureau of Mines Bulletin 680 1985.
- [14] I. Wierzba, B. B. Ale, Rich Flammability Limits of Fuel Mixtures Involving Hydrogen at Elevated Temperatures, *International Journal of Hydrogen Energy*, 25 (2000) 75-80
- [15] I. Wierzba, G. A. Karim, H. Cheng, The Flammability of Rich Gaseous Fuel Mixtures Including Those Containing Propane in Air, *Journal of Hazardous materials*, 20 (1988) 303-312.
- [16] D. S. Burgess, A. L. Furno, J. M. Kuchta, K. E. Mura, Flammability of Mixed Gases, U.S. Bureau of Mines, Report of Investigations RI 8709, 1982.
- [17] K. L. Cashdollar, I. A. Zlochower, G. M. Green, R.A. Thomas, M. Hertzberg, Flammability of Methane, Propane, and Hydrogen Gases, *Journal of Loss Prevention in the Process Industries*, 13 (2000) 327-340.

- [18] W. Grosshandler, M. Donnelly, C. Womeldorf, Lean Flammability Limit as a Fundamental Refrigerant Property: Phase III, DOE/CE/23810-98, 1998.
- [19] Y. Ju, H. Guo, K. Maruta, Determination of Burning Velocity and Flammability Limit of Methane/Air Mixture Using Counterflow Flames, *Jpn. J. Appl. Phys.*, 38 (1999) 961-967.
- [20] M. Subramanya, D. S. Davu, A. Choudhuri, Experimental Investigation on the Flame Extinction Limit of Fuel Blends, 43<sup>rd</sup> AIAA Aerospace Science Meeting and Exhibit, Reno, Nevada 2005.
- [21] H. F. Coward, G. W. Jones, C. G. Dunkle, B. E. Hess, The Explosibility of Methane and Natural Gas, *Mining and Metallurgical Investigations, Bulletin* 30, (1929) 17-41.
- [22] ASTM E 681-01, Standard Test Method for Concentration Limits of Flammability of Chemicals (vapors and gases), 2001.
- [23] ASTM E 2079-01, Standard test methods for Limiting Oxygen (oxidant) Concentration in Gases and Vapors, 2001.
- [24] ASTM E 918-83, Standard Practice for Determining Limits of Flammability of Chemicals at Elevated Temperature and Pressure, 1999.
- [25] V. Schroder, M. Molnarne, Flammability of Gas Mixtures Part 1: Fire Potential, *Journal of Hazardous Materials A121* (2005) 37-44.
- [26] E. W. Heinonen, R. E. Tapscott, F. R. Crawford, Methods Development for Measuring and Classifying Flammability/Combustibility of Refrigerants,

- DOE/CE/23810-50, NMERI, The University of New Mexico, Albuquerque, 1994.
- [27] G. W. Jones, E. S. Harris, W. E. Miller, Explosive Properties of Acetone-Air Mixtures, U.S. Bureau of Mines, Technical Paper 544, 1933.
- [28] L. A. Medard, Accidental Explosions, Volume 1, John Wiley & Sons, New York, NY, 1989 147-151.
- [29] C. Mashuga, "Determination of the Combustion Behavior for Pure Components and Mixtures Using a 20 liter Sphere," Ph.D. Dissertation, Department of Chemical Engineering, Michigan Technical University, 1999.
- [30] Thermometrics, NTC application notes,  
<http://thermometrics.com/assets/images/ntcnotes.pdf>, (1999).
- [31] Efundu Engineering Fundamentals, Wheatstone Bridges: Introduction,  
[http://efunda.com/designstandards/sensors/methods/wheatstone\\_bridge.cfm](http://efunda.com/designstandards/sensors/methods/wheatstone_bridge.cfm), (2006).
- [32] J. R. Farr, M. H. Jawad, Guidebook for the Design of ASME Section VIII Pressure Vessels, ASME Press, New York, 1997.

## VITA

NAME: Wun K. Wong

ADDRESS: Department of Chemical Engineering, Texas A&M University,  
TAMU 3122, College Station, TX 77843-3122

EMAIL ADDRESS: wunwong@hotmail.com

EDUCATION: B.A. Chemistry, Harvey Mudd College, 2000